

MarkTune: Improving the Quality-Detectability Trade-off in Open-Weight LLM Watermarking

Yizhou Zhao¹ Zhiwei Steven Wu² Adam Block³

¹University of Pennsylvania

²Carnegie Mellon University

³Columbia University

December 4, 2025

Abstract

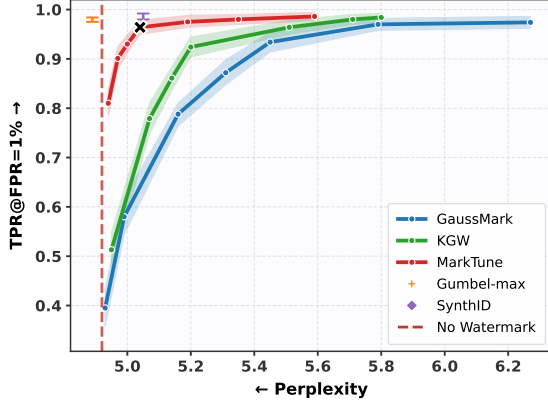
Watermarking aims to embed hidden signals in generated text that can be reliably detected when given access to a secret key. Open-weight language models pose acute challenges for such watermarking schemes because the inference-time interventions that dominate contemporary approaches cannot be enforced once model weights are public. Existing watermarking techniques for open-weight models, such as the recently proposed GAUSSMARK, typically rely on small modifications to model weights, which can yield signals detectable to those equipped with a secret key, but achieving detection power comparable to inference-time watermarks generally requires weight perturbations that noticeably reduce generation quality. We introduce MARKTUNE, a theoretically principled, on-policy fine-tuning framework that treats the GAUSSMARK signal as a reward while simultaneously regularizing against degradation in text quality. We derive MARKTUNE as an improvement on GAUSSMARK and demonstrate that MARKTUNE consistently improves the quality-detectability trade-off over GAUSSMARK by steering finer-grained, watermark-aware weight updates within the model’s representation space while preserving generation quality. Empirically, we show that MARKTUNE pushes the quality-detectability frontier of GAUSSMARK close to that of inference-time watermarking, remains robust to paraphrasing and fine-tuning attacks, and exhibits strong generalization: a model fine-tuned on one dataset retains substantial watermark detection power on unseen datasets. Together, these results establish MARKTUNE as a general strategy for embedding robust, high-quality watermarks into open-weight LMs.

1 Introduction

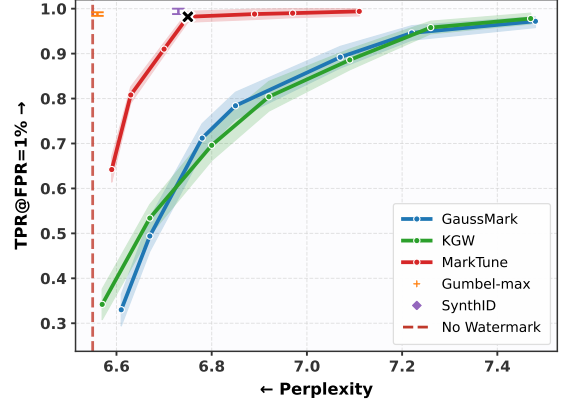
Open-weight Language Models (LMs) are growing in prevalence due to their rapidly improving capabilities [17, 19, 51]. As open-weight models continue to be deployed, they raise significant concerns about potential misuse on top of the pre-existing societal impacts introduced by closed-weight models. As such, it is critical to develop techniques to ensure appropriate usage that are effective on open-weight models and are sufficiently practical so as to be widely adopted. In this work, we focus on the specific task of *watermarking* LM output, i.e., introducing an almost imperceptible signal into generated text that, when given access to a secret key, can be reliably detected in a statistically valid manner. Watermarking is critical to establish trust that a given piece of text is or is not generated by an LM, which is a necessary prerequisite in a number of societal applications, including academic integrity [27, 32, 42], misinformation mitigation [24, 45, 53], and intellectual property protection [25, 34, 50].

Emails: yzzhao@sas.upenn.edu, zstevenwu@cmu.edu, and adam.block@columbia.edu.

Code is available at <https://github.com/zhyzmth/MarkTune-LLM-Watermarking>.



(a) Qwen3-4B, $T=0.7$, length=200 tokens.



(b) Llama2-7B, $T=1.0$, length=200 tokens.

Figure 1: Trade-off between detectability (TPR@1% FPR) and text quality (Perplexity) across various watermarking schemes. Inference-time watermarking methods (KGW [28], Gumbel-max [1], SynthID [10]) modify only the sampling process and are shown here for reference, as they are not applicable in open-weight settings. Model-embedded watermarking methods (GAUSSMARK [4] and our MARKTUNE) embed the watermark directly into the model weights. MARKTUNE substantially improves the trade-off over GAUSSMARK and achieves performance comparable to inference-time watermarking methods. The black “x” marks the MARKTUNE configuration used in Section 4.

Previous work has posed watermarking as a statistical hypothesis testing problem [4, 23, 31], where a joint distribution is assumed over the text and some watermarking key: in the null hypothesis, the key and text are independent (meaning the text is unwatermarked), while in the alternative hypothesis, the key and text have some statistically detectable relation (meaning the text is watermarked). The goal of a watermarking scheme, then, is to design a mechanism for generating text given a key such that the null and alternative hypotheses can be reliably distinguished, subject to quality constraints on the generated text itself. These quality constraints are often formalized as strict, information-theoretic notions of non-distortion [8, 21, 30] (e.g., the marginal distributions of watermarked and unwatermarked text should be close in total variation distance). In order to satisfy these stringent guarantees while maintaining high detectability, many current approaches to watermarking LMs involve interventions at *inference time* [10, 21, 28, 30, 47, 48], by subtly changing the sampling itself to introduce a watermark signal. While this approach can be effective when the model is accessed only through a generation API, in the case of open-weight models, the provider has no control over a user’s generation pipeline and, as such, cannot guarantee that such a watermark will be present in generated text. This problem motivates the need for watermarking techniques specifically designed for open-weight models, where the watermark is embedded directly into the model weights themselves and thus does not require a user to apply a specific decoding approach. Several distortionary watermarking schemes have been proposed that maintain high text quality [4, 7, 18, 49], suggesting that information-theoretic notions of distortion are conservative measures of text quality.

One recently introduced watermarking scheme that intervenes at the level of weights instead of during inference is GAUSSMARK [4], which adds a small amount of Gaussian noise to a subset of the weight matrices, subtly shifting the distribution of generated text in a manner detectable when given access to the added Gaussian noise. In [4], the authors demonstrated that if the variance of the added noise is sufficiently small, and the parameters are carefully chosen, then the text distribution can be modified so as to achieve nontrivial detectability with no loss of text quality. Moreover, [15] demonstrated that GAUSSMARK is at least somewhat robust to a number of simple fine-tuning attacks that a user may apply in an attempt to remove the

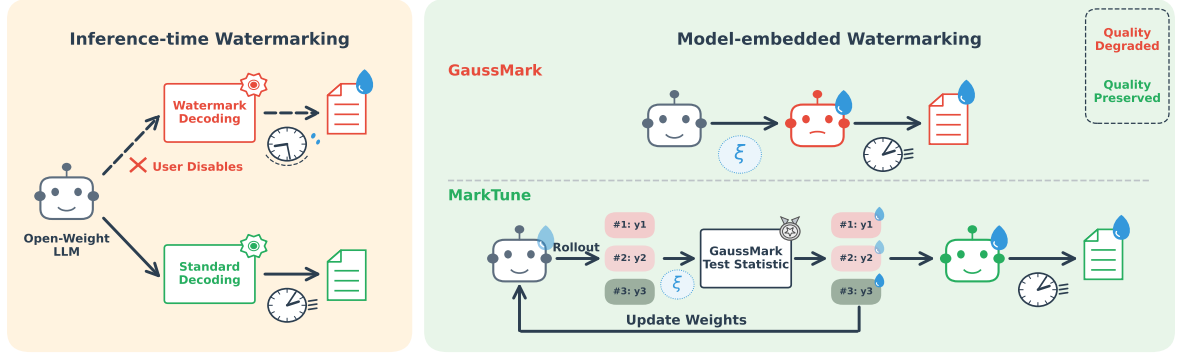


Figure 2: Overview of our framework compared to prior work [1, 4, 10, 28]. **Left:** Inference-time watermarking schemes break down on open-weight LLMs because users can disable the decoding algorithm, and these methods often introduce substantial generation latency (⌚ indicates no latency; ⌚ indicates extra latency). **Right:** Our approach, MARKTUNE, treats the GAUSSMARK test statistic as a reward and performs on-policy fine-tuning to embed a highly detectable yet quality-preserving watermark signal into the model’s weights.

watermark from the weights of the model. Taken together, these results suggest that GAUSSMARK is a promising approach, but it remains unclear how close GAUSSMARK lies to the optimal quality-detectability frontier, and whether this trade-off can be further improved through more fine-grained and adaptive modifications to the model weights. We thus ask—*Can we design a watermarking scheme for open-weight LMs that preserves text quality and downstream task performance, achieves detection power comparable to inference-time watermarking, and remains robust to realistic text-editing and fine-tuning attacks?*

Our contribution. In this work, we answer the above question in the affirmative by proposing MARKTUNE, a theoretically principled on-policy fine-tuning framework that improves the trade-off between quality and detectability of GAUSSMARK to match that of inference-time watermarking schemes. The core idea is simple: treat the GAUSSMARK test statistic as a reward during fine-tuning while regularizing the model to preserve text quality. This procedure enables the GAUSSMARK signal to be embedded in an adaptive and robust manner within the model’s overparameterized representation space. Our framework also preserves the statistical validity of detection, ensuring that the resulting test retains the same false-positive guarantees as the underlying scheme. Through extensive experiments and ablations, we show that MARKTUNE consistently improves the quality-detectability trade-off for GAUSSMARK across datasets and tasks, achieves detection performance close to inference-time watermarking while maintaining generation quality and downstream task performance, and remains robust to realistic text-editing and fine-tuning attacks.

Related Work LM text watermarking schemes can be broadly categorized into two families: *inference-time* watermarking and *model-embedded* watermarking. Distortionary inference-time schemes modify the sampling process—for example, by biasing next-token sampling toward a partitioned “green list” [28, 54]. Although these methods provide statistical guarantees, they introduce noticeable distortion in generated text and are vulnerable to realistic paraphrasing attacks [26, 39]. In contrast, nondistortionary inference-time schemes embed watermark signals by influencing the pseudorandom number generator used in next-token sampling while preserving the original distribution. For instance, [1] and [30] draw independent pseudorandom variables and generate tokens using deterministic decoders based on the Gumbel-max trick and inverse transform sampling. Similarly, [48] and [47] propose unbiased variants of the KGW watermark [28]

by introducing decoding algorithms based on maximal coupling and reweighting strategies, respectively. However, these approaches are not yet suitable for large-scale LM deployment due to their generation latency [4] and the fact that the joint distribution is often not preserved under key collisions [46]. More recently, [10] introduced a tournament-based watermarking, which achieves high detection power with minimal latency overhead. However, maintaining text quality in this setting requires storage that scales linearly with the number of generated tokens, making it impractical for large production systems.

Model-embedded watermarking can be divided into two categories: training-based schemes [18, 49] and weight-editing schemes [4, 7]. These approaches embed the watermark signal directly into model weights, making them naturally suitable for open-weight LMs while incurring neither generation latency nor additional storage overhead. However, training-based schemes remain limited in learnability and generalization across tasks [18] and lack rigorous guarantees on the statistical validity of detection [49]. Weight-editing schemes, in contrast, either require modifications to standard model architectures [7] or suffer from computationally intensive hyperparameter searches and limited advancement in balancing text quality with detection performance [4].

2 Preliminaries

A language model is any conditional distribution mapping a *prompt* $x \in \mathcal{X}$ (the space of prompts) to a distribution over responses $y \in \mathcal{Y}$ (the space of responses), i.e. a function $p : \mathcal{X} \rightarrow \Delta(\mathcal{Y})$. As is common in language modeling, we will generally consider *autoregressive generation*, where there is some vocabulary set \mathcal{V} and both \mathcal{X} and \mathcal{Y} are subsets of \mathcal{V}^* . In this case, the model generates a response one token at a time by sampling $y_1 \sim p(\cdot|x)$, then $y_t \sim p(\cdot|x, y_1, \dots, y_{t-1})$ and concatenating the output tokens to form a response. As we are chiefly concerned with transformer instantiations of language models, we generally parameterize the model by some set of weights $\Theta \subset \mathbb{R}^d$ and write p_θ for the resulting model. Typically, in the case of transformers, $\theta \in \Theta$ can be thought of as the concatenation of a large number of high-dimensional matrices, one for each layer of the transformer.

Hypothesis testing. As in [4, 23, 31], we formalize the notion of watermarking as a statistical hypothesis testing problem. Recall that a hypothesis testing problem consists of an observation space $\Xi \times \mathcal{Y}$ and two disjoint collections of distributions on the observation space, \mathbf{H}_0 and \mathbf{H}_A . A test is a (possibly randomized) function $\phi : \Xi \times \mathcal{Y} \rightarrow \{0, 1\}$, where $\phi(\xi, y) = 1$ indicates that the observation (ξ, y) provides sufficient evidence to suggest that it was not sampled from any distribution in \mathbf{H}_0 . The test is said to have level α if the false positive rate, the probability that $\phi = 1$ even when (ξ, y) is sampled from an element of the null hypothesis, is at most α . The power of the test, $1 - \beta$, is the probability that $\phi = 1$ when (ξ, y) is truly sampled from an element of the alternative hypothesis. Clearly we wish to have a test with both α and β as small as possible.

Weight-editing watermarking. There are three phases in a weight-editing watermarking scheme: embedding, generation and detection. Formally, let Ξ denotes the key space with an associated distribution ρ . Given a language model p_θ , we first sample a key $\xi \sim \rho$ and obtain a watermarked model $p_{\theta(\xi)}$ by applying a weight-editing algorithm $\mathcal{A} : \Theta \times \Xi \rightarrow \Theta$, so that $\theta(\xi) = \mathcal{A}(\theta, \xi)$. The watermarked text is then generated by sampling $y \sim p_{\theta(\xi)}(\cdot | x)$ using a prompt x . Detection is formulated as a hypothesis test, where $\mathbf{H}_0 = \{\rho \otimes q | q \in \Delta(\mathcal{Y})\}$ denotes the set of joint distributions under which the key ξ and the text y are independent, and \mathbf{H}_A corresponds to the joint distribution induced by the watermarking generation process.¹

¹As stated, the detector has access to the prompt x used to generate y . In practice, this is of course not the case and **our empirical results do not rely on this access**.

The fundamental statistical difficulty of distinguishing \mathbf{H}_A from \mathbf{H}_0 is governed by the total variation (TV) distance between the induced distributions under the two hypotheses [23], whose square is upper bounded by the well-known KL divergence up to a constant by Pinsker’s inequality [5].

GAUSSMARK. In this work we focus on improving GAUSSMARK [4], a recently proposed weight-editing watermarking scheme. Given a language model $p_\theta : \mathcal{X} \rightarrow \Delta(\mathcal{Y})$, GAUSSMARK partitions the weights as $\theta = (\theta_{\text{wm}}, \theta_0)$, where θ_{wm} (with dimension d_r) is the subset of model weights modified to embed the watermark, and θ_0 the remaining weights. The base model p_θ is stored as a fixed reference model for later detection. To embed a watermark, GAUSSMARK samples the key $\xi_\sigma \sim \mathcal{N}(0, \sigma^2 \mathbb{I}_{d_r})$ and obtains watermarked model $p_{\theta(\xi_\sigma)}$ with $\theta(\xi_\sigma) = (\theta_{\text{wm}} + \xi_\sigma, \theta_0)$, i.e., it perturbs the selected weights with a small amount of Gaussian noise and leaves the others unchanged. To detect the watermark, GAUSSMARK uses the following test statistic:

$$\psi(y, \xi_\sigma | x) = \frac{\langle \xi_\sigma, \nabla_{\theta_{\text{wm}}} \log p_\theta(y | x) \rangle}{\sigma \|\nabla_{\theta_{\text{wm}}} \log p_\theta(y | x)\|_2}. \quad (1)$$

Intuitively, this statistic measures the alignment between the secret key ξ_σ and the gradient of the reference model with respect to the watermarked weights. Under \mathbf{H}_0 , ξ_σ is independent of the text y , so $\psi(y, \xi_\sigma | x)$ follows a standard normal distribution and a test of level α can be constructed by thresholding the statistic at the inverse Gaussian CDF (denoted by Φ^{-1}) at $1 - \alpha$.

3 MARKTUNE: On-Policy Fine-Tuning with Watermark Signal Rewards

In this section, we introduce our proposed watermarking scheme, MARKTUNE, a theoretically principled approach that enhances the quality-detectability trade-off of GAUSSMARK through on-policy fine-tuning with watermark signal rewards. To motivate MARKTUNE, we first present the following result on the distortion introduced by GAUSSMARK.

Proposition 1. *Let p_θ be a language model with parameters $\theta = (\theta_{\text{wm}}, \theta_0) \in \Theta$, where $\theta_{\text{wm}} \in \mathbb{R}^{d_r}$ is the subset of parameters to which the GAUSSMARK is applied. Assume that the map $\theta' \mapsto \text{D}_{\text{KL}}(p_{\theta'}(\cdot | x) \| p_\theta(\cdot | x))$ is twice continuously differentiable with uniformly bounded Hessian.² If $\xi_\sigma \sim \mathcal{N}(0, \sigma^2 \mathbb{I}_{d_r})$ is Gaussian and $\theta(\xi_\sigma) = (\theta_{\text{wm}} + \xi_\sigma, \theta_0)$, then for any prompt x there is a constant C depending on the Hessian bound such that*

$$\mathbb{E}_{\xi_\sigma} \left[\text{D}_{\text{KL}}(p_{\theta(\xi_\sigma)}(\cdot | x) \| p_\theta(\cdot | x)) \right] \leq C \sigma^2 d_r. \quad (2)$$

Because the TV distance from the base model characterizes watermark strength and is upper bounded by the KL divergence via Pinsker’s inequality, Proposition 1 (whose formal proof is deferred to Appendix B.1) appears to suggest a fundamental quality-detectability trade-off for GAUSSMARK: enhancing watermark detectability by increasing σ or the watermark subspace dimension d_r inevitably increases the KL-based upper bound on the resulting quality distortion.

Nevertheless, we argue that such pessimism is overstated for two reasons. First, the base model p_θ should not be regarded as an oracle that perfectly characterizes the high-quality text but instead is a learned model with imperfections. Consequently, closeness to the base model is not a necessary condition for achieving high-quality generation; rather, one should prefer closeness to some optimal distribution p_{θ^*} that better expresses the true distribution of observed text. Such intuition is expressed in Figure 3, where the base model p_θ is suboptimal compared to the high-quality reference model p_{θ^*} ; while GAUSSMARK attempts to maintain generation

²This condition can be relaxed to local continuity and bounding of the Hessian at the cost of conditioning on the high probability event that $\theta(\xi)$ remains in this neighborhood.

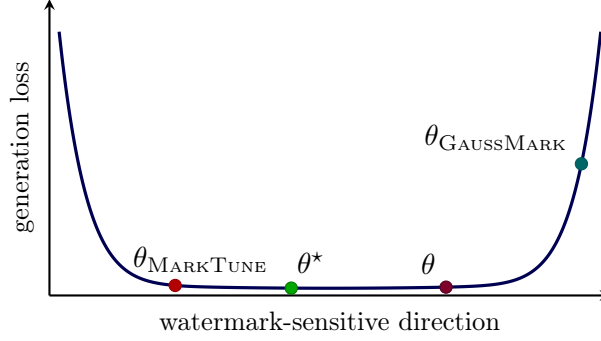


Figure 3: Stylized one-dimensional landscape along a watermark-sensitive direction. Both $\theta_{\text{GAUSSMARK}}$ and θ_{MARKTUNE} lie at nontrivial distances from the base model θ along this direction, leading to significant watermark detectability, but θ_{MARKTUNE} resides within the flat high-quality basin around θ^* and therefore incurs substantially less quality degradation than $\theta_{\text{GAUSSMARK}}$.

quality by remaining close to θ , our proposed method MARKTUNE (outlined below) instead seeks parameters that remain close to θ^* .

Second, KL divergence is a particularly stringent measure of distributional distortion, as it upper-bounds worst-case deviations across all possible events, which is far stricter than what is required for human-perceived quality. Indeed, modern LMs are heavily over-parameterized, and their loss landscapes are known to contain broad, flat basins [6]. Consequently, given a base model p_θ , there typically exist alternative weight configurations p_{θ^*} that exhibit a significant TV distance from p_θ but that yield essentially the same generation quality on general or domain-specific tasks. This perspective is also depicted in Figure 3, where both GAUSSMARK and MARKTUNE achieve similar watermark strength (denoted by the horizontal distance from θ) but our proposed MARKTUNE maintains better generation quality by remaining in the basin of the high-quality reference model θ^* .

Design motivation. Inspired by the success of Reinforcement Learning from Human Feedback (RLHF) [35] and Reinforcement Learning with Verifiable Rewards (RLVR) [19] in enhancing LLM capabilities, we propose MARKTUNE, an on-policy fine-tuning framework that uses the GAUSSMARK test statistic as its reward. Unlike the rewards in RLHF and RLVR, which are typically produced by trained reward models, domain-specific verifiers, or gold-standard solutions, this test statistic is an intrinsic quantity that can be easily computed using a watermark key. Following prior work, we include a regularization term in the optimization objective to preserve generation quality. However, unlike conventional RL objectives [19, 35, 40], which regularize using the KL divergence between the trained model and the base model, we instead use the cross-entropy on alternative high-quality human text or the KL divergence to an oracle model that accurately reflects the target language distribution yet remains distinguishable from the base model in total variation. This choice provides a larger search space for watermark-aware weight updates and influences the training dynamics to evolve in favor of watermark-sensitive directions along which generation quality decays relatively slowly, thereby yielding a more favorable quality-detectability trade-off.

Optimization with dual objectives. Given a base language model p_θ with $\theta = (\theta_{\text{wm}}, \theta_0)$ and a watermark key $\xi_\sigma \sim \mathcal{N}(0, \sigma^2 \mathbb{I}_{d_r})$ for small σ , MARKTUNE first applies a GAUSSMARK soft activation $\theta(\xi_\sigma) = (\theta_{\text{wm}} + \xi_\sigma, \theta_0)$, resulting in a weak watermark signal that maintains generation quality. The base model p_θ is subsequently fixed, and the training objective is given by

$$\max_{\theta(\xi_\sigma)} \mathbb{E}_{x \sim \mathcal{D}, y \sim p_{\theta(\xi_\sigma)}(\cdot|x)} \left[\text{sg} \left(\frac{\langle \xi_\sigma, \nabla_{\theta_{\text{wm}}} \log p_\theta(y) \rangle}{\sigma \|\nabla_{\theta_{\text{wm}}} \log p_\theta(y)\|_2} \right) \right] - \lambda \mathcal{L}_{\text{reg}}(\theta(\xi_\sigma); x, y), \quad (3)$$

Algorithm 1 MARKTUNE with GAUSSMARK soft activation

- 1: **Input:** Language model p_θ with $\theta = (\theta_{\text{wm}}, \theta_0)$, strength $\sigma > 0$, text dataset \mathcal{D} , regularization coefficient $\lambda > 0$.
 - 2: Sample watermark key $\xi_\sigma \sim \mathcal{N}(0, \sigma^2 \mathbb{I}_{d_r})$.
 - 3: Inject GAUSSMARK perturbation to obtain $\theta(\xi_\sigma) = (\theta_{\text{wm}} + \xi_\sigma, \theta_0)$.
 - 4: Conduct GRPO Algorithm 2 for $\theta(\xi_\sigma)$ to obtain $\theta^*(\xi_\sigma)$ via optimizing the objective (3).
 - 5: **Output:** Watermarked weights $\theta^*(\xi_\sigma)$.
-

where the first term is the watermark signal reward $\mathcal{R}_{\text{wm}}(y; \xi_\sigma)$, formulated using the GAUSSMARK test statistic.³ The operator $\text{sg}(\cdot)$ denotes stop-gradient: the gradient $\nabla_{\theta_{\text{wm}}} \log p_\theta(y)$ is computed on a fixed p_θ and treated as constant with respect to $\theta(\xi_\sigma)$, so no backpropagation passes through it. The term \mathcal{L}_{reg} is a regularization term, which can be either the cross-entropy loss $\mathcal{L}_{\text{ce}} = -\frac{1}{T} \sum_{t=1}^T \log p_{\theta(\xi_\sigma)}(x_t | x_{<t})$ or the KL divergence to an oracle model $\mathcal{L}_{\text{kl}} = \text{D}_{\text{KL}}(p_{\theta(\xi_\sigma)}(y | x) \| p_{\text{oracle}}(y | x))$ ⁴. $\lambda > 0$ denotes a hyperparameter that balances the watermark reward against the regularization on text quality degradation. By rewarding generated samples $y \sim p_{\theta(\xi_\sigma)}(\cdot | x)$ that produce stronger watermark signals, while penalizing deviations from high-quality text through \mathcal{L}_{reg} , this dual-objective, on-policy fine-tuning framework improves the quality-detectability trade-off of vanilla MARKTUNE. The high-level procedure of MARKTUNE is summarized in Algorithm 1. For practical implementation, we employ GRPO [41] to optimize the overall objective (3), with algorithm details provided in Appendix A.

Remark 1. We emphasize that, in principle, MARKTUNE can serve as a general on-policy fine-tuning framework for improving the quality-detectability trade-off of any weight-editing watermarking by replacing the first term in (3) with the corresponding test statistic or any computable detection rule as the reward. We choose GAUSSMARK in this work due to the theoretical motivation outlined below.

Type I error control. For watermark detection, we inherit the procedure in GAUSSMARK. Since the generated text y remains independent of ξ_σ under \mathbf{H}_0 , Proposition 2, whose proof is in Appendix B.2, provides rigorous statistical guarantees on the false positive rate.

Proposition 2. Let $\alpha \in (0, 1)$, and $\tau_\alpha := \Phi^{-1}(1 - \alpha)$ where Φ is the CDF of the standard normal distribution. Then, for any $y \in \mathcal{Y}$, the test $\mathbb{I}\left\{\frac{\langle \xi_\sigma, \nabla_{\theta_{\text{wm}}} \log p_\theta(y) \rangle}{\sigma \|\nabla_{\theta_{\text{wm}}} \log p_\theta(y)\|_2} \geq \tau_\alpha\right\}$ has level α .

Informal analysis. We can gain intuition for why MARKTUNE is superior to GAUSSMARK in the simple linear-softmax regime that is often considered as an analytically tractable proxy for gaining insight and intuition in language modeling settings [4, 13, 22]. In this setting, we suppose that the “language model” $p_\theta(y|x) \propto \exp(\langle \theta, \Phi(x, y) \rangle)$, where $\Phi(x, y)$ denotes a fixed feature map; such a setting is partially motivated by supposing that all except for the last layer of a transformer are frozen. Suppose that θ^* denotes the parameter that yields the best possible language model, while θ denotes the base language model. Let \mathcal{L}_{reg} be crossentropy on text generated from p_{θ^*} and noting that this is the same as $\text{D}_{\text{KL}}(p_{\theta'} \| p_{\theta^*})$ up to an additive constant independent of θ' , we see that the regularized objective in (3) becomes a KL-regularized policy optimization problem. Thus, applying the standard Donsker-Varadhan reparameterization trick [11, 37], we see that if trained to completion (and ignoring the rescaling in (3) for the sake of simplicity), $p_{\theta_{\text{MARKTUNE}}}(y|x) \propto p_{\theta^*}(y|x) \cdot \exp(\langle \xi, \Phi(x, y) \rangle)$. Thus, under the linear-softmax assumption, it holds that $p_{\theta_{\text{MARKTUNE}}}(y|x) \propto \exp(\langle \theta^* + \xi, \Phi(x, y) \rangle)$ in contradistinction to GAUSSMARK, which satisfies $p_{\theta_{\text{GAUSSMARK}}}(y|x) \propto \exp(\langle \theta + \xi, \Phi(x, y) \rangle)$. Thus, at a high level, MARKTUNE is applying

³We ignore the prompt x to match the real-world detection setting.

⁴We conduct an ablation study on the selection of regularization term in Section 4.4.

GAUSSMARK to the *optimal parameter* instead of that of the base model, which explains why MARKTUNE is capable of improving on GAUSSMARK with respect to the quality-detectability frontier. In this way, the analyses of the *statistical power* of MARKTUNE follow precisely from those of GAUSSMARK contained in [4].

We further make the above intuition concrete in Appendix C. In a neighborhood of the high-quality distribution p_{θ^*} , one can identify a deviation $\delta\theta$ along the watermark-sensitive direction such that the watermark reward, and thus the mean of the test statistic, increases at *first order* in $\kappa = \frac{1}{\lambda}$, while the resulting increase in cross-entropy (or KL) to p_{θ^*} appears only at *second order*. This provides additional theoretical insights into why MARKTUNE can achieve an adaptive and quality-preserving watermarking of model weights.

4 Experiments

In this section, we evaluate the performance of MARKTUNE on two LMs and datasets to demonstrate its broad applicability across models and its generalizability to different tasks. Specifically, we verify its efficacy along four key dimensions: 1) comparison of generation quality and watermark detection performance against existing watermarking schemes, including both inference-time and model-embedded approaches; 2) impact of watermarking on downstream task performance; 3) robustness to text-editing attacks; and 4) robustness to fine-tuning attacks. **Throughout all experiments, we use *prompt-agnostic* detection, mirroring practical deployment scenarios where the prompt is unknown to the detector.** We instantiate the MARKTUNE detector with the statistic in (1) evaluated without the prompt,

$$\psi(y, \xi_\sigma) = \frac{\langle \xi_\sigma, \nabla_{\theta_{\text{wm}}} \log p_\theta(y) \rangle}{\sigma \|\nabla_{\theta_{\text{wm}}} \log p_\theta(y)\|_2},$$

where the gradient is taken with respect to the log-likelihood of the entire text under the base model p_θ , treating y as a standalone sequence. Further implementation details are provided in Appendix D.

4.1 Experimental Setup

Models and datasets. In our evaluation, we consider two open-weight LLMs—Qwen3-4B [52] and Llama2-7B [44]. The former is relatively new, while the latter is widely used in prior watermarking work [18, 30, 47, 49, 55]. Following the guidelines in [44, 52], we use a sampling temperature of 0.7 for Qwen3-4B and 1.0 for Llama2-7B to ensure high-quality generation.

We evaluate watermarking performance on two text generation tasks: 1) text completion and 2) question answering. For text completion, we use the **RealNewsLike** split of the **C4** dataset [38] to serve as prompts. For long-form question answering, we use the **ELI5** dataset [12], where the model generates detailed responses to the questions. For both tasks, we randomly sample 500 prompts and generate responses of 200 tokens. For MARKTUNE fine-tuning, we use a subset of **OpenWebText** [16] as the training corpus, with prompt lengths ranging from 64 to 256 tokens for on-policy sampling. **We emphasize that the dataset on which we train MARKTUNE is disjoint and very different from the evaluation datasets, demonstrating its ability to generalize generation of watermarked text across domains.**

Baselines and metrics. We benchmark our method against a range of representative watermarking schemes, including inference-time methods KGW [28] with two different hyperparameter settings (KGW-1 and KGW-2), OpenAI’s Gumbel-max [1], Google’s SynthID [10], and model-embedded methods such as KGW-D [18], which imitates KGW via logit distillation, and GAUSSMARK [4]. We omit RL-based watermarking [49] because we were unable to train it to achieve non-trivial detection power across datasets under multinomial sampling. To ensure a fair

Table 1: Text generation quality and watermark detectability for different methods. Best performances among model-embedded watermarks are shown in **bold**.

Method	C4-RealNewsLike					ELI5				
	AUC \uparrow	TPR \uparrow	PPL \downarrow	Seq-rep-3 \downarrow	MAUVE \uparrow	AUC \uparrow	TPR \uparrow	PPL \downarrow	Seq-rep-3 \downarrow	MAUVE \uparrow
Qwen3-4B, T=0.7										
No Watermark	0.500	0.010	4.92 _{1.34}	0.04	0.98	0.500	0.010	2.67 _{0.94}	0.03	0.94
KGW-1	0.996	0.964	5.51 _{1.56}	0.04	0.98	0.971	0.710	3.04 _{1.12}	0.04	0.92
KGW-2	1.000	0.998	6.65 _{1.91}	0.04	0.96	0.996	0.988	3.69 _{1.51}	0.03	0.87
Gumbel-max	0.995	0.980	4.89 _{2.07}	0.18	0.74	0.991	0.938	2.71 _{1.01}	0.13	0.77
SynthID	0.996	0.986	5.05 _{1.54}	0.04	0.96	0.993	0.946	2.76 _{0.95}	0.06	0.91
KGW-D	0.981	0.762	5.54 _{1.53}	0.04	0.98	0.941	0.542	3.09 _{1.17}	0.04	0.92
GaussMark	0.983	0.788	5.16 _{1.54}	0.04	0.98	0.979	0.734	2.83 _{1.07}	0.03	0.93
MarkTune	0.995	0.964	5.04_{1.37}	0.03	0.97	0.996	0.942	2.78_{1.03}	0.03	0.93
Llama2-7B, T=1.0										
No Watermark	0.500	0.010	6.55 _{1.80}	0.01	0.98	0.500	0.010	7.86 _{2.23}	0.02	0.97
KGW-1	0.991	0.886	7.09 _{2.04}	0.02	0.96	0.993	0.946	8.47 _{2.39}	0.04	0.94
KGW-2	0.997	0.996	8.14 _{2.36}	0.01	0.95	1.000	1.000	9.61 _{2.68}	0.03	0.91
Gumbel-max	0.997	0.988	6.56 _{1.84}	0.14	0.86	0.998	0.994	7.98 _{2.29}	0.18	0.81
SynthID	0.995	0.994	6.73 _{1.94}	0.03	0.94	0.997	0.988	8.06 _{2.41}	0.09	0.89
KGW-D	0.945	0.582	7.04 _{1.98}	0.02	0.98	0.969	0.754	8.53 _{2.41}	0.05	0.96
GaussMark	0.974	0.712	6.78 _{1.91}	0.01	0.98	0.958	0.622	8.13_{2.15}	0.02	0.94
MarkTune	0.997	0.982	6.75_{1.96}	0.01	0.96	0.993	0.930	8.19_{2.27}	0.01	0.96

detectability comparison, we select hyperparameters that allow each watermarking scheme to achieve nontrivial detection performance while incurring minimal degradation in text quality.

We evaluate both watermark detectability and generated text quality. For watermark detectability, we report the true positive rate (TPR) at a fixed false positive rate of 1% (TPR@FPR=1%) as well as the area under the ROC curve (AUC). To assess generation quality, we compute perplexity (PPL) using Qwen3-8B and Llama2-13B as oracle language models corresponding to each evaluated model. To measure repetitiveness, we compute Seq-rep-3, defined as the average repetition rate of duplicate 3-grams in a sequence. We also report MAUVE scores to quantify the distributional similarity between model generations and human text [36].

4.2 Main Results

Table 1 reports the generation quality and detection performance of different watermarking methods across models and datasets. We observe that **MARKTUNE consistently outperforms other model-embedded watermarking approaches in detectability while introducing only minimal degradation in text quality** (all three quality metrics remain close to the unwatermarked baseline). It also matches the performance of inference-time watermarking methods, achieving comparable generation quality and detection strength. KGW attains high detectability but at the cost of substantial perplexity degradation. In contrast, Gumbel-max generally offers strong detectability and low perplexity, but suffers from notable repetitiveness due to its deterministic decoding procedure. SynthID generally performs well in both detectability and generation quality.

Figure 1 illustrates the quality-detectability trade-off for all watermarking schemes on **C4-RealNewsLike**.⁵ For each method, we sweep a scheme-specific parameter that controls the watermark strength to generate the trade-off curve, except for Gumbel-max and SynthID, which are non-distortionary and therefore yield a single TPR-PPL point. Compared with GAUSSMARK and KGW, MARKTUNE achieves a significantly more favorable trade-off, yielding higher detection rates for the same level of perplexity distortion.

⁵We omit the trade-off curve of KGW-D since its performance is upper bounded by KGW.

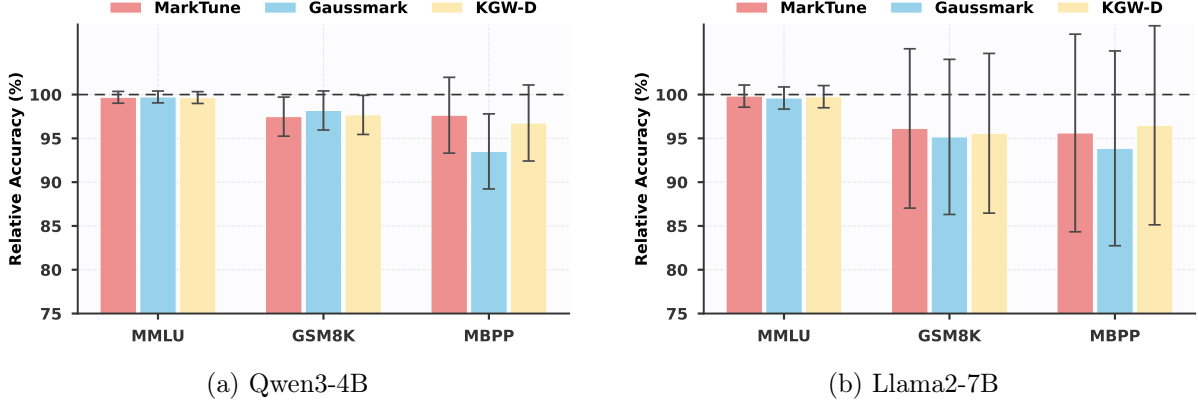


Figure 4: Relative downstream task accuracy compared to unwatermarked models across the general, math, and coding benchmarks.

Impact on downstream tasks performance. Because watermarking strategies alter the output distributions of LLMs, it is essential to ensure that the utility of the underlying model is not compromised. Although the results in Table 1 indicate minimal degradation in generation quality—measured by perplexity, Seq-rep-3, and MAUVE—recent work [2, 4, 10] has shown that such metrics do not reliably predict the performance degradation introduced by watermarking on downstream tasks. Therefore, we further evaluate the watermarked models on downstream tasks using the Language Model Evaluation Harness [14] across three benchmarks: MMLU [20] for general knowledge and reasoning, GSM8K [9] for mathematical problem solving, and MBPP [3] for coding tasks. Figure 4 reports the accuracy of three model-embedded watermarking schemes on these benchmarks, relative to the unwatermarked model. On the MMLU benchmark, all methods exhibit negligible accuracy degradation, indicating that they preserve the model’s general capabilities. On the GSM8K and MBPP benchmarks, MARKTUNE ranks first or second, substantially improving over vanilla GAUSSMARK, especially on MBPP. We attribute this to the fact that MARKTUNE more effectively guides the training dynamics toward “directions” that simultaneously enhance the watermark signal and preserve utility, starting from only a slight weight perturbation. In contrast, GAUSSMARK requires a much larger perturbation to produce a nontrivial watermark signal, which can negatively affect downstream performance. We provide watermarked examples in Appendix F for generation quality illustration beyond these quantitative metrics.

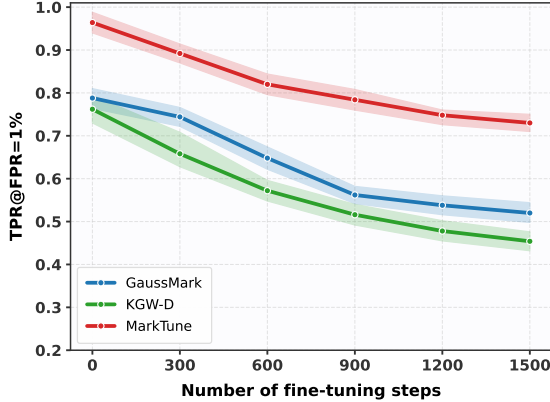
4.3 Robustness Evaluation

Robustness to text-editing attacks. Text editing is common in practical LLM usage and can weaken watermark signals. We evaluate watermark robustness against four widely used text-editing attacks: word deletion, synonym substitution, paraphrasing, and roundtrip translation. For the first two attacks, we randomly select a fraction of watermarked tokens and either delete them or replace them with synonyms sampled from WordNet [33]. For paraphrasing, we apply two Dipper [29] configurations that vary in lexical and order diversity. We additionally include a more challenging paraphrasing attack by performing roundtrip translation: we translate the watermarked text into French using `Helsinki-NLP/opus-mt-tc-big-en-fr` and translate it back into English using `Helsinki-NLP/opus-mt-tc-big-fr-en` [43].

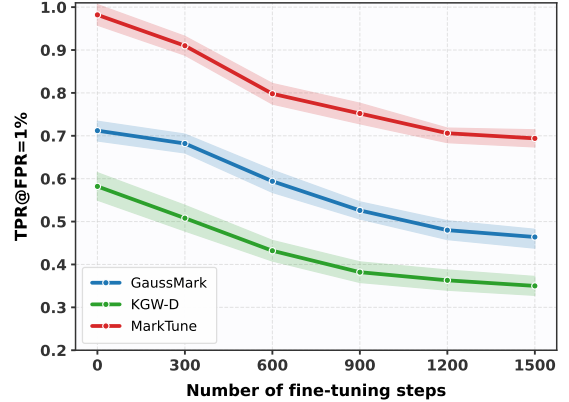
For word deletion and synonym substitution attacks, KGW-D often performs strongly among model-embedded watermarking methods, as it distilled from the one-token-prefix KGW watermark. While MARKTUNE shows consistent improvement over GAUSSMARK, but still exhibits notable decay in watermark signal under higher modification rates. *However, we emphasize that such token-level attacks are relatively crude and do not constitute realistic threat*

Table 2: Watermark detectability under text-editing and paraphrasing attacks for different methods on **C4-RealNewsLike**. “Del- n ” and “Sub- n ” denote attacks that delete or substitute a proportion of n tokens, respectively. “Dipper-1” refers to Dipper paraphrasing with lexical and order diversity set to 20, while “Dipper-2” uses a diversity level of 60. “Translate” denotes the roundtrip translation attack described in Section 4.3. Best performances among model-embedded watermarks are shown in **bold**.

Method	Del-0.2		Del-0.5		Sub-0.2		Sub-0.5		Dipper-1		Dipper-2		Translate	
	AUC \uparrow	TPR \uparrow	AUC \uparrow	TPR \uparrow	AUC \uparrow	TPR \uparrow	AUC \uparrow	TPR \uparrow	AUC \uparrow	TPR \uparrow	AUC \uparrow	TPR \uparrow	AUC \uparrow	TPR \uparrow
Qwen3-4B, T=0.7														
KGW-1	0.881	0.330	0.617	0.040	0.873	0.324	0.638	0.048	0.771	0.142	0.573	0.026	0.831	0.242
KGW-2	0.975	0.746	0.697	0.082	0.986	0.826	0.747	0.106	0.884	0.372	0.616	0.038	0.928	0.552
Gumbel-max	0.993	0.948	0.778	0.162	0.993	0.922	0.840	0.348	0.945	0.748	0.721	0.146	0.955	0.846
SynthID	0.987	0.890	0.780	0.094	0.986	0.846	0.834	0.182	0.941	0.576	0.700	0.074	0.968	0.818
KGW-D	0.947	0.582	0.851	0.196	0.939	0.578	0.837	0.190	0.855	0.274	0.589	0.030	0.912	0.404
GaussMark	0.908	0.366	0.622	0.048	0.919	0.384	0.775	0.100	0.915	0.438	0.795	0.138	0.948	0.574
MarkTune	0.921	0.484	0.744	0.068	0.948	0.552	0.783	0.110	0.977	0.852	0.851	0.254	0.973	0.858
Llama2-7B, T=1.0														
KGW-1	0.853	0.232	0.581	0.024	0.878	0.300	0.638	0.030	0.757	0.116	0.551	0.014	0.777	0.146
KGW-2	0.975	0.712	0.711	0.060	0.980	0.756	0.772	0.126	0.862	0.322	0.614	0.032	0.922	0.448
Gumbel-max	0.993	0.924	0.790	0.224	0.993	0.950	0.862	0.296	0.950	0.700	0.711	0.148	0.961	0.796
SynthID	0.979	0.774	0.777	0.114	0.987	0.862	0.843	0.140	0.943	0.552	0.710	0.084	0.949	0.612
KGW-D	0.914	0.410	0.803	0.148	0.887	0.406	0.759	0.144	0.814	0.238	0.590	0.026	0.889	0.324
GaussMark	0.835	0.242	0.617	0.036	0.853	0.228	0.759	0.098	0.857	0.240	0.687	0.060	0.925	0.436
MarkTune	0.928	0.506	0.783	0.080	0.944	0.578	0.809	0.122	0.961	0.836	0.859	0.270	0.966	0.834



(a) Qwen3-4B



(b) Llama2-7B

Figure 5: Detectability (TPR@1%FPR) decay under LoRA fine-tuning attack.

models, as they substantially degrade text quality. To illustrate this degradation, in Table 7 (deferred to the appendix for space), we report the perplexity of texts after applying various editing attacks. We observe that token-level attacks substantially degrade quality, whereas paraphrasing attacks—against which MARKTUNE is notably robust—preserve text quality while reducing the detectability of alternative watermarks. A more meaningful evaluation focuses on paraphrasing attacks. Across all paraphrasing settings, our method outperforms all watermarking baselines—including strong inference-time approaches—demonstrating its robustness and promising applicability under realistic adversarial deployment.

Robustness to fine-tuning attack. Given the open-weight deployment setting, we also evaluate the robustness of weight-embedded watermarks to fine-tuning attacks. With the growing adoption of LoRA as a PEFT technique, we consider an adversary who attempts to remove the

Table 3: Ablation study on regularization hyperparameters. “Base” denotes the watermarked trained using MARKTUNE without a regularization term. Configuration highlighted in **bold** indicates Pareto-optimal performance.

Method	AUC \uparrow	TPR \uparrow	PPL \downarrow	Seq-rep-3 \downarrow	MAUVE \uparrow
Base	0.999	0.992	5.88 _{1.55}	0.06	0.89
+ CE-0.005	0.997	0.976	5.35 _{1.43}	0.05	0.94
+ CE-0.01	0.995	0.964	5.04_{1.37}	0.03	0.97
+ CE-0.05	0.989	0.902	4.97 _{1.31}	0.03	0.97
+ KL-0.001	0.997	0.986	5.69 _{1.56}	0.06	0.93
+ KL-0.005	0.993	0.930	5.36 _{1.41}	0.06	0.95
+ KL-0.01	0.986	0.854	5.13 _{1.32}	0.04	0.97

Table 4: Ablation study on GRPO sampling hyperparameters group size (“G”) and temperature (“T”). Configuration highlighted in **bold** indicates Pareto-optimal performance.

G	T	AUC \uparrow	TPR \uparrow	PPL \downarrow	Seq-rep-3 \downarrow	MAUVE \uparrow
8	0.7	0.995	0.964	5.04_{1.37}	0.03	0.97
4	0.7	0.992	0.900	5.07 _{1.38}	0.03	0.98
16	0.7	0.996	0.968	5.11 _{1.42}	0.03	0.97
8	0.5	0.983	0.820	4.98 _{1.28}	0.06	0.92
8	1.0	0.992	0.940	6.21 _{2.26}	0.03	0.94

watermark by further fine-tuning the model on **OpenWebText** using LoRA, following the setup in prior work [15]. As shown in Figure 5, although MARKTUNE enhances the watermark via fine-grained on-policy weight updates, it does not exhibit a faster TPR decay rate than the other two methods. Owing to its strong initial watermark signal, it retains substantial detection power even after 1500 fine-tuning steps, in contrast to GAUSSMARK and KGW-D.

4.4 Ablation Study

We conduct an ablation study on Qwen3-4B to investigate how different components of MARKTUNE influence the quality-detectability trade-off. Empirically, we find that the regularization term and its coefficient, as well as the GRPO sampling hyperparameters, are the primary factors shaping MARKTUNE’s performance.

Regularization term and coefficient λ . Table 3 highlights the effect of the regularization term. Without regularization, the model aggressively amplifies the watermark signal but at a cost to generation quality. Introducing cross-entropy or KL regularization restores perplexity and diversity while maintaining strong detectability, with cross-entropy with $\lambda = 0.01$ offering the most balanced performance and thus serving as our default choice in Section 4.2 and 4.3. This shows that MARKTUNE’s gains over vanilla GAUSSMARK do not come from simply increasing watermark strength, but from guiding weight updates in a watermark-sensitive direction while staying close to the underlying high-quality text generation distribution.

GRPO sampling hyperparameters. As for the impact of GRPO sampling hyperparameters on MARKTUNE, Table 4 indicates that the method is generally insensitive to the choice of group size. In practice, a group size of 8 provides the best balance between performance and computational cost. The sampling temperature should follow the model-specific settings

commonly used for high-quality text generation, as deviations from these values either reduce output diversity or increase perplexity.

5 Conclusion

We introduced MARKTUNE, a practical and theoretically grounded on-policy fine-tuning framework for watermarking open-weight language models. By optimizing a dual objective that combines a watermark-signal reward derived from the GAUSSMARK test statistic with a regularization term on generation quality, MARKTUNE enables watermark-aware yet quality-preserving exploration in the over-parameterized representation space. Extensive empirical evaluations across models and datasets show that MARKTUNE consistently improves the quality-detectability trade-off of vanilla GAUSSMARK, reaching performance close to non-distortive inference-time watermarking while preserving downstream task performance. The approach is also robust to paraphrasing and fine-tuning attacks and generalizes well to unseen data. These results suggest that MARKTUNE offers a flexible and effective framework for embedding reliable, high-quality watermarks into open-weight language models.

References

- [1] Scott Aaronson. Watermarking of large language models. <https://simons.berkeley.edu/talks/scott-aaronson-ut-austin-openai-2023-08-17>, August 2023.
- [2] Anirudh Ajith, Sameer Singh, and Danish Pruthi. Downstream trade-offs of a family of text watermarks. In *Findings of the Association for Computational Linguistics: EMNLP 2024*, pages 14039–14053, 2024.
- [3] Jacob Austin, Augustus Odena, Maxwell Nye, Maarten Bosma, Henryk Michalewski, David Dohan, Ellen Jiang, Carrie Cai, Michael Terry, Quoc Le, et al. Program synthesis with large language models. *arXiv preprint arXiv:2108.07732*, 2021.
- [4] Adam Block, Ayush Sekhari, and Alexander Rakhlin. Gaussmark: A practical approach for structural watermarking of language models. In *International Conference on Machine Learning*, 2025.
- [5] Clément L Canonne. A short note on an inequality between KL and TV. *arXiv preprint arXiv:2202.07198*, 2022.
- [6] Huanran Chen, Yinpeng Dong, Zeming Wei, Yao Huang, Yichi Zhang, Hang Su, and Jun Zhu. Understanding pre-training and fine-tuning from loss landscape perspectives. *arXiv preprint arXiv:2505.17646*, 2025.
- [7] Miranda Christ, Sam Gunn, Tal Malkin, and Mariana Raykova. Provably robust watermarks for open-source language models. *arXiv preprint arXiv:2410.18861*, 2024.
- [8] Miranda Christ, Sam Gunn, and Or Zamir. Undetectable watermarks for language models. In *The Thirty Seventh Annual Conference on Learning Theory*, pages 1125–1139. PMLR, 2024.
- [9] Karl Cobbe, Vineet Kosaraju, Mohammad Bavarian, Mark Chen, Heewoo Jun, Lukasz Kaiser, Matthias Plappert, Jerry Tworek, Jacob Hilton, Reiichiro Nakano, et al. Training verifiers to solve math word problems. *arXiv preprint arXiv:2110.14168*, 2021.
- [10] Sumanth Dathathri, Abigail See, Sumedh Ghaisas, Po-Sen Huang, Rob McAdam, Johannes Welbl, Vandana Bachani, Alex Kaskasoli, Robert Stanforth, Tatiana Matejovicova, et al. Scalable watermarking for identifying large language model outputs. *Nature*, 634(8035):818–823, 2024.
- [11] Monroe D Donsker and SR Srinivasa Varadhan. Asymptotic evaluation of certain markov process expectations for large time, I. *Communications on pure and applied mathematics*, 28(1):1–47, 1975.
- [12] Angela Fan, Yacine Jernite, Ethan Perez, David Grangier, Jason Weston, and Michael Auli. ELI5: Long Form Question Answering. In *Proceedings of the 57th Annual Meeting of the Association for Computational Linguistics*, pages 3558–3567, 2019.
- [13] Dylan J Foster, Zakaria Mhammedi, and Dhruv Rohatgi. Is a good foundation necessary for efficient reinforcement learning? the computational role of the base model in exploration. *arXiv preprint arXiv:2503.07453*, 2025.
- [14] Leo Gao, Jonathan Tow, Stella Biderman, Sid Black, Anthony DiPofi, Charles Foster, Laurence Golding, Jeffrey Hsu, Kyle McDonell, Niklas Muennighoff, et al. A framework for few-shot language model evaluation. *Zenodo*, 2021.

- [15] Thibaud Gloaguen, Nikola Jovanović, Robin Staab, and Martin Vechev. Towards watermarking of open-source llms. *arXiv preprint arXiv:2502.10525*, 2025.
- [16] Aaron Gokaslan, Vanya Cohen, Ellie Pavlick, and Stefanie Tellex. OpenWebText Corpus. <http://Skylion007.github.io/OpenWebTextCorpus>, 2019.
- [17] Aaron Grattafiori, Abhimanyu Dubey, Abhinav Jauhri, Abhinav Pandey, Abhishek Kadian, Ahmad Al-Dahle, Aiesha Letman, Akhil Mathur, Alan Schelten, Alex Vaughan, et al. The llama 3 herd of models. *arXiv preprint arXiv:2407.21783*, 2024.
- [18] Chenchen Gu, Xiang Lisa Li, Percy Liang, and Tatsunori Hashimoto. On the learnability of watermarks for language models. In *International Conference on Learning Representations*, 2024.
- [19] Daya Guo, Dejian Yang, Haowei Zhang, Junxiao Song, Ruoyu Zhang, Runxin Xu, Qihao Zhu, Shirong Ma, Peiyi Wang, Xiao Bi, et al. Deepseek-r1: Incentivizing reasoning capability in llms via reinforcement learning. *arXiv preprint arXiv:2501.12948*, 2025.
- [20] Dan Hendrycks, Collin Burns, Steven Basart, Andy Zou, Mantas Mazeika, Dawn Song, and Jacob Steinhardt. Measuring massive multitask language understanding. *arXiv preprint arXiv:2009.03300*, 2020.
- [21] Zhengmian Hu, Lichang Chen, Xidong Wu, Yihan Wu, Hongyang Zhang, and Heng Huang. Unbiased watermark for large language models. In *International Conference on Learning Representations*, 2024.
- [22] Audrey Huang, Adam Block, Dylan J Foster, Dhruv Rohatgi, Cyril Zhang, Max Simchowitz, Jordan T Ash, and Akshay Krishnamurthy. Self-improvement in language models: The sharpening mechanism. In *The Thirteenth International Conference on Learning Representations*, 2025.
- [23] Baihe Huang, Hanlin Zhu, Banghua Zhu, Kannan Ramchandran, Michael I Jordan, Jason D Lee, and Jiantao Jiao. Towards optimal statistical watermarking. *arXiv preprint arXiv:2312.07930*, 2023.
- [24] Md Rafiqul Islam, Shaowu Liu, Xianzhi Wang, and Guandong Xu. Deep learning for misinformation detection on online social networks: a survey and new perspectives. *Social Network Analysis and Mining*, 10(1):82, 2020.
- [25] Yongqi Jiang, Yansong Gao, Chunyi Zhou, Hongsheng Hu, Anmin Fu, and Willy Susilo. Intellectual property protection for deep learning model and dataset intelligence. *arXiv preprint arXiv:2411.05051*, 2024.
- [26] Nikola Jovanović, Robin Staab, and Martin Vechev. Watermark stealing in large language models. In *International Conference on Machine Learning*, 2024.
- [27] Enkelejda Kasneci, Kathrin Sekler, Stefan Küchemann, Maria Bannert, Daryna Dementieva, Frank Fischer, Urs Gasser, Georg Groh, Stephan Günemann, Eyke Hüllermeier, et al. Chatgpt for good? on opportunities and challenges of large language models for education. *Learning and individual differences*, 103:102274, 2023.
- [28] John Kirchenbauer, Jonas Geiping, Yuxin Wen, Jonathan Katz, Ian Miers, and Tom Goldstein. A watermark for large language models. In *International Conference on Machine Learning*, 2023.

- [29] Kalpesh Krishna, Yixiao Song, Marzena Karpinska, John Wieting, and Mohit Iyyer. Paraphrasing evades detectors of ai-generated text, but retrieval is an effective defense. *Advances in Neural Information Processing Systems*, 36:27469–27500, 2023.
- [30] Rohith Kuditipudi, John Thickstun, Tatsunori Hashimoto, and Percy Liang. Robust Distortion-free Watermarks for Language Models. *Transactions on Machine Learning Research*, 2024.
- [31] Xiang Li, Feng Ruan, Huiyuan Wang, Qi Long, and Weijie J Su. A statistical framework of watermarks for large language models: Pivot, detection efficiency and optimal rules. *The Annals of Statistics*, 53(1):322–351, 2025.
- [32] Silvia Milano, Joshua A McGrane, and Sabina Leonelli. Large language models challenge the future of higher education. *Nature Machine Intelligence*, 5(4):333–334, 2023.
- [33] George A Miller. Wordnet: a lexical database for English. *Communications of the ACM*, 38(11):39–41, 1995.
- [34] Claudio Novelli, Federico Casolari, Philipp Hacker, Giorgio Spedicato, and Luciano Floridi. Generative AI in EU law: Liability, privacy, intellectual property, and cybersecurity. *Computer Law & Security Review*, 55:106066, 2024.
- [35] Long Ouyang, Jeffrey Wu, Xu Jiang, Diogo Almeida, Carroll Wainwright, Pamela Mishkin, Chong Zhang, Sandhini Agarwal, Katarina Slama, Alex Ray, et al. Training language models to follow instructions with human feedback. In *Advances in neural information processing systems*, 2022.
- [36] Krishna Pillutla, Swabha Swayamdipta, Rowan Zellers, John Thickstun, Sean Welleck, Yejin Choi, and Zaid Harchaoui. Mauve: Measuring the gap between neural text and human text using divergence frontiers. In *Advances in Neural Information Processing Systems*, 2021.
- [37] Rafael Rafailov, Archit Sharma, Eric Mitchell, Christopher D Manning, Stefano Ermon, and Chelsea Finn. Direct preference optimization: Your language model is secretly a reward model. In *Advances in neural information processing systems*, 2023.
- [38] Colin Raffel, Noam Shazeer, Adam Roberts, Katherine Lee, Sharan Narang, Michael Matena, Yanqi Zhou, Wei Li, and Peter J Liu. Exploring the limits of transfer learning with a unified text-to-text transformer. *Journal of machine learning research*, 21(140):1–67, 2020.
- [39] Saksham Rastogi and Danish Pruthi. Revisiting the robustness of watermarking to paraphrasing attacks. *arXiv preprint arXiv:2411.05277*, 2024.
- [40] John Schulman, Filip Wolski, Prafulla Dhariwal, Alec Radford, and Oleg Klimov. Proximal policy optimization algorithms. *arXiv preprint arXiv:1707.06347*, 2017.
- [41] Zhihong Shao, Peiyi Wang, Qihao Zhu, Runxin Xu, Junxiao Song, Xiao Bi, Haowei Zhang, Mingchuan Zhang, YK Li, Yang Wu, et al. Deepseekmath: Pushing the limits of mathematical reasoning in open language models. *arXiv preprint arXiv:2402.03300*, 2024.
- [42] Chris Stokel-Walker. AI bot ChatGPT writes smart essays-should professors worry? *Nature News*, 2022.
- [43] Jörg Tiedemann, Mikko Aulamo, Daria Bakshandaeva, Michele Boggia, Stig-Arne Grönroos, Tommi Nieminen, Alessandro Raganato, Yves Scherrer, Raúl Vázquez, and Sami Virpioja. Democratizing neural machine translation with OPUS-MT. *Language Resources and Evaluation*, 58(2):713–755, 2024.

- [44] Hugo Touvron, Louis Martin, Kevin Stone, Peter Albert, Amjad Almahairi, Yasmine Babaei, Nikolay Bashlykov, Soumya Batra, Prajjwal Bhargava, Shruti Bhosale, et al. Llama 2: Open foundation and fine-tuned chat models. *arXiv preprint arXiv:2307.09288*, 2023.
- [45] Laura Weidinger, John Mellor, Maribeth Rauh, Conor Griffin, Jonathan Uesato, Po-Sen Huang, Myra Cheng, Mia Glaese, Borja Balle, Atoosa Kasirzadeh, et al. Ethical and social risks of harm from language models. *arXiv preprint arXiv:2112.04359*, 2021.
- [46] Yihan Wu, Ruibo Chen, Zhengmian Hu, Yanshuo Chen, Junfeng Guo, Hongyang Zhang, and Heng Huang. Distortion-free watermarks are not truly distortion-free under watermark key collisions. *arXiv preprint arXiv:2406.02603*, 2024.
- [47] Yihan Wu, Zhengmian Hu, Hongyang Zhang, and Heng Huang. DipMark: A stealthy, efficient and resilient watermark for large language models. *arXiv preprint arXiv:2310.07710*, 2023.
- [48] Yangxinyu Xie, Xiang Li, Tanwi Mallick, Weijie Su, and Ruixun Zhang. Debiasing watermarks for large language models via maximal coupling. *Journal of the American Statistical Association*, pages 1–21, 2025.
- [49] Xiaojun Xu, Yuanshun Yao, and Yang Liu. Learning to watermark llm-generated text via reinforcement learning. *arXiv preprint arXiv:2403.10553*, 2024.
- [50] Zhenhua Xu, Xubin Yue, Zhebo Wang, Qichen Liu, Xixiang Zhao, Jingxuan Zhang, Wenjun Zeng, Wengpeng Xing, Dezhang Kong, Changting Lin, et al. Copyright protection for large language models: A survey of methods, challenges, and trends. *arXiv preprint arXiv:2508.11548*, 2025.
- [51] An Yang, Anfeng Li, Baosong Yang, Beichen Zhang, Binyuan Hui, Bo Zheng, Bowen Yu, Chang Gao, Chengen Huang, Chenxu Lv, et al. Qwen3 technical report. *arXiv preprint arXiv:2505.09388*, 2025.
- [52] An Yang, Anfeng Li, Baosong Yang, Beichen Zhang, Binyuan Hui, Bo Zheng, Bowen Yu, Chang Gao, Chengen Huang, Chenxu Lv, et al. Qwen3 technical report. *arXiv preprint arXiv:2505.09388*, 2025.
- [53] Rowan Zellers, Ari Holtzman, Hannah Rashkin, Yonatan Bisk, Ali Farhadi, Franziska Roesner, and Yejin Choi. Defending against neural fake news. In *Advances in neural information processing systems*, 2019.
- [54] Xuandong Zhao, Prabhanjan Vijendra Ananth, Lei Li, and Yu-Xiang Wang. Provable robust watermarking for AI-generated text. In *International Conference on Learning Representations*, 2024.
- [55] Xuandong Zhao, Lei Li, and Yu-Xiang Wang. Permute-and-Flip: An optimally stable and watermarkable decoder for LLMs. In *The Thirteenth International Conference on Learning Representations*, 2024.

Algorithm 2 GRPO for MARKTUNE

```
1: Input: initial policy model  $p_{\theta(\xi_\sigma)}$ ; watermark signal reward  $\mathcal{R}_{\text{wm}}(\cdot; \xi_\sigma)$ ; text dataset  $\mathcal{D}$ ;
   hyperparameters  $\varepsilon, \lambda, T_1, T_2$ .
2: Initialize: Set  $p_\theta \leftarrow p_{\theta(\xi_\sigma)}$ .
3: for step = 1, ...,  $T_1$  do
4:   Sample a batch  $\mathcal{D}_b \subset \mathcal{D}$ .
5:    $p_{\theta_{\text{old}}} \leftarrow p_\theta$ .
6:   for each prompt  $x \in \mathcal{D}_b$  do
7:     Sample  $G$  outputs  $\{y_j\}_{j=1}^G \sim p_{\theta_{\text{old}}}(\cdot | x)$ .
8:     Compute rewards  $\{r_j\}_{j=1}^G$  using  $\mathcal{R}_{\text{wm}}$ .
9:     Compute  $\hat{A}_j$  for response  $y_j$  via group-relative advantage Eq.(4).
10:  end for
11:  for iteration = 1, ...,  $T_2$  do
12:    Update  $p_\theta$  by maximizing the GRPO objective Eq.(5).
13:  end for
14: end for
15: Output:  $p_\theta$ .
```

A Practical Implementation of MARKTUNE

To optimize the objective in Eq.(3), we use the GRPO [41] algorithm. This choice is motivated by the fact that Eq.(3) cannot be directly optimized due to its dependence on sampled outputs $y \sim p_{\theta(\xi_\sigma)}$. GRPO is a critic-free, on-policy policy-gradient method that replaces the learned value baseline in PPO with a group-relative baseline computed from multiple samples per prompt, which makes it well-suited for optimizing our objective.

For each prompt from a batch $x \sim \mathcal{D}_b$, we sample a group of responses $\{y_j\}_{j=1}^G$ from the current policy and compute their watermark signal rewards $\mathbf{r} = \{r_j\}_{j=1}^G$. The advantage for sample j is normalized within the group:

$$\hat{A}_j = (r_j - \text{mean}(\mathbf{r})) / \text{std}(\mathbf{r}) \quad (4)$$

The policy update follows a clipped objective based on the importance ratio $\rho_j = \frac{p_\theta(y_j | x)}{p_{\theta_{\text{old}}}(y_j | x)}$, maximizing $\mathbb{E} \left[\min(\rho_j \hat{A}_j, \text{clip}(\rho_j, 1 - \epsilon, 1 + \epsilon) \hat{A}_j) \right]$ together with a specified language modeling regularization term. The overall GRPO objective is give by

$$\begin{aligned} \mathcal{J}(\theta) = & \mathbb{E}_{x \sim \mathcal{D}, \{y_j\}_{j=1}^G \sim p_\theta(\cdot | x)} \\ & \frac{1}{G} \sum_{j=1}^G \min \left[\frac{p_\theta(y_j | x)}{p_{\theta_{\text{old}}}(y_j | x)} \hat{A}_j, \text{clip} \left(\frac{p_\theta(y_j | x)}{p_{\theta_{\text{old}}}(y_j | x)}, 1 - \varepsilon, 1 + \varepsilon \right) \hat{A}_j \right] - \lambda \mathcal{L}_{\text{reg}}(\theta; x, \{y_j\}_{j=1}^G). \end{aligned} \quad (5)$$

See Algorithm 2 for the detailed implementation of GRPO.

B Theorems and Proofs

B.1 Proof of Proposition 1

Proof. Given a prompt x , we write $p_\theta(\cdot | x)$ by p_θ for simplicity. Then we denote KL divergence induced by GAUSSMARK with $\xi_\sigma \sim \mathcal{N}(0, \sigma^2 \mathbb{I}_{d_r})$ as $D(\xi_\sigma) := \text{KL} \left(p_{\theta(\xi_\sigma)} \parallel p_\theta \right) \geq 0$. Since $D(0) = 0$ and its gradient vanishes at the global minimum $\left(\nabla_{\xi_\sigma} D(\xi_\sigma) \big|_{\xi_\sigma=0} = 0 \right)$, its Taylor

expansion around $\xi_\sigma = 0$ begins at second order:

$$D(\xi_\sigma) = \frac{1}{2} \xi_\sigma^\top \mathcal{I}(\theta_{\text{wm}}) \xi_\sigma + o(\|\xi_\sigma\|^2), \quad \mathcal{I}(\theta_{\text{wm}}) := \nabla_{\xi_\sigma}^2 D(\xi_\sigma)|_{\xi_\sigma=0},$$

where $\mathcal{I}(\theta_{\text{wm}}) \in \mathbb{R}^{d_r \times d_r}$ is the Fisher information matrix. Each diagonal entry $\mathcal{I}_{jj}(\theta_{\text{wm}})$ of $\mathcal{I}(\theta_{\text{wm}})$ represents the Fisher information of j -th component $\theta_{\text{wm}}^{(j)}$ of θ_{wm} and measures how much information a single model response y provides about the specific parameter component $\theta_{\text{wm}}^{(j)}$:

$$\mathcal{I}_{jj}(\theta_{\text{wm}}) = \mathbb{E}_{y \sim p_\theta(\cdot|x)} \left[\left(\frac{\partial \log p_\theta(y|x)}{\partial \theta_{\text{wm}}^{(j)}} \right)^2 \right].$$

Then we take the expectation of this approximation with respect to the distribution of ξ_σ :

$$\begin{aligned} \mathbb{E}[D(\xi_\sigma)] &= \mathbb{E} \left[\frac{1}{2} \xi_\sigma^\top \mathcal{I}(\theta_{\text{wm}}) \xi_\sigma + o(\|\xi_\sigma\|^2) \right] \\ &= \frac{1}{2} \mathbb{E} \left[\text{tr}(\mathcal{I}(\theta_{\text{wm}}) \xi_\sigma \xi_\sigma^\top) \right] + o(\sigma^2 d_r) \\ &= \frac{1}{2} \text{tr} \left\{ \mathcal{I}(\theta_{\text{wm}}) \mathbb{E} \left[\xi_\sigma \xi_\sigma^\top \right] \right\} + o(\sigma^2 d_r) \\ &= \frac{\sigma^2}{2} \text{tr}(\mathcal{I}(\theta_{\text{wm}})) + o(\sigma^2 d_r). \end{aligned}$$

For a well-defined model, there exists a model-dependent constant capturing the local Lipschitz sensitivity of the map $\theta_{\text{wm}} \mapsto p_{(\theta_{\text{wm}}, \theta_0)}(\cdot|x)$. In the worst case this constant can scale with a network Lipschitz factor (e.g., products of layer operator norms), which may grow exponentially in depth. In practice this is milder: restricting watermarking to later layers reduces the effective sensitivity, and empirical results from [4] demonstrate that the scaling can be much more moderate. Therefore, it is natural to make an assumption that there exists a model-dependent constant $C(p_\theta) > 0$ such that

$$\mathcal{I}_{jj}(\theta_{\text{wm}}) \leq C(p_\theta).$$

Then we have $\mathbb{E}[D(\xi_\sigma)] \leq \frac{C(p_\theta)\sigma^2 d_r}{2}$. Writing it formally gives us

$$\mathbb{E}_{\xi_\sigma} \left[\text{D}_{\text{KL}} \left(p_{\theta(\xi_\sigma)}(\cdot|x) \parallel p_\theta(\cdot|x) \right) \right] \leq C \sigma^2 d_r,$$

where $C > 0$ depends only on the local curvature of this KL map around θ . \square

B.2 Proof of Proposition 2

Proof. Under the null hypothesis \mathbf{H}_0 , for any $y \in \mathcal{Y}$, the key and the generated text y are independent of each other, i.e., $(\xi_\sigma, y) \sim \mathcal{N}(0, \sigma^2 \mathbb{I}_{d_r}) \otimes q$ for some $q \in \Delta(\mathcal{Y})$. Therefore, the level of the test is given by

$$\begin{aligned} \Pr_{\mathbf{H}_0}(\psi(y; \xi_\sigma) = 1) &= \mathbb{E}_{\xi_\sigma \sim \mathcal{N}(0, \sigma^2 \mathbb{I}_{d_r}), y \sim q} \left[\mathbb{I} \left\{ \frac{\langle \xi_\sigma, \nabla_{\theta_{\text{wm}}} \log p_\theta(y) \rangle}{\sigma \|\nabla_{\theta_{\text{wm}}} \log p_\theta(y)\|_2} \geq \tau_\alpha \right\} \right] \\ &= \mathbb{E}_{y \sim q} \left[\Pr_{\xi_\sigma} \left(\frac{\langle \xi_\sigma, \nabla_{\theta_{\text{wm}}} \log p_\theta(y) \rangle}{\sigma \|\nabla_{\theta_{\text{wm}}} \log p_\theta(y)\|_2} \geq \tau_\alpha \right) \right] \\ &= \mathbb{E}_{y \sim q} \left[\Pr_{\xi_\sigma}(\psi(y; \xi_\sigma) \geq \tau_\alpha) \right] \\ &= 1 - \Phi(\tau_\alpha) = \alpha, \end{aligned}$$

where the last line is based on

$$\psi(y; \xi_\sigma) = \frac{\langle \xi_\sigma, \nabla_{\theta_{\text{wm}}} \log p_\theta(y) \rangle}{\sigma \|\nabla_{\theta_{\text{wm}}} \log p_\theta(y)\|_2} \sim \mathcal{N}(0, 1)$$

for any vector $\nabla_{\theta_{\text{wm}}} \log p_\theta(y)$. The last equality is derived by plugging in $\tau_\alpha = \Phi^{-1}(1 - \alpha)$. \square

C A Stylized Linear-Softmax Analysis of MARKTUNE

In this section we provide a stylized analysis of how MARKTUNE can improve the quality-detectability trade-off. The goal is not to reproduce all realistic training dynamics, but rather to study the local geometry of the objective optimized in the main text, within an idealized linear-softmax model.

Model and notation. Let $\theta \in \mathbb{R}^d$ denote the full set of model weights. For a fixed watermark key ξ , a weight-editing scheme such as GAUSSMARK produces an initial watermarked weight $\theta(\xi)$ (Here we omit ξ 's dependence on σ for simplicity); MARKTUNE then fine-tunes $\theta(\xi)$ by optimizing a reward-regularized objective.

For the analysis, we adopt a standard linear-softmax setting:

$$p_\theta(y | x) \propto \exp\{\langle \theta, \Phi(x, y) \rangle\}, \quad (6)$$

where $\Phi(x, y) \in \mathbb{R}^d$ is a fixed feature map that encodes the prompt-response pair.

Let $p^*(\cdot | x)$ denote a high-quality target conditional distribution (e.g., the population language distribution or an oracle model). We assume that p^* is realized within the linear-softmax family by a weight θ^* :

$$p^*(y | x) = p_{\theta^*}(y | x) \propto \exp\{\langle \theta^*, \Phi(x, y) \rangle\}.$$

The population cross entropy risk of a weight θ relative to p^* is

$$\mathcal{L}(\theta) := \mathbb{E}_x \mathbb{E}_{y \sim p^*(\cdot | x)} [-\log p_\theta(y | x)]. \quad (7)$$

As in the main text, the watermark reward is induced by the GAUSSMARK test statistic (For stylized analysis we include the prompt x in the test statistic). Let q'_θ be the fixed reference model used for detection, and define

$$h(x, y; \xi) := \left\langle \xi, \nabla_{\theta_{\text{wm}}} \log q'_\theta(y | x) \right\rangle, \quad (8)$$

where θ_{wm} denotes the watermarked block of the reference model parameters. The unnormalized watermark reward of θ is then

$$\mathcal{R}(\theta) := \mathbb{E}_x \mathbb{E}_{y \sim p_\theta(\cdot | x)} [h(x, y; \xi)]. \quad (9)$$

The stylized MARKTUNE objective in this setting is

$$J(\theta) = \mathcal{R}(\theta) - \lambda \mathcal{L}(\theta),$$

where $\lambda > 0$ is a regularization coefficient controlling the trade-off between watermark reward and regularization term. For the sake of analysis, we assume that the GAUSSMARK-soft-activated weight $\theta(\xi)$ lies in a neighborhood of θ^* , and study the local geometry of J around the high-quality target weight θ^* .

Goal. We want to show that, in a neighborhood of θ^* , there exists a perturbation $\delta\theta$ in the full parameter space such that the adjusted weight

$$\theta_{\text{MARKTUNE}} := \theta^* + \delta\theta$$

satisfies, for a small scalar $\kappa = 1/\lambda > 0$:

- (i) the cross entropy relative to p^* changes only at *second order*, $\mathcal{L}(\theta_{\text{MARKTUNE}}) - \mathcal{L}(\theta^*) = \Theta(\kappa^2)$,
- (ii) the watermark reward increases at *first order*, $\mathcal{R}(\theta_{\text{MARKTUNE}}) - \mathcal{R}(\theta^*) = \Theta(\kappa)$,

This implies that, under $p_{\theta_{\text{MARKTUNE}}}$ the (normalized) detection statistic exhibits a mean shift of order κ , improving detection power at fixed false positive rate, while the degradation in generation quality is quadratically smaller.

Assumptions. We adopt the following standard local assumptions for linear soft-max models.

(A1) *Smoothness.* The map $\theta \mapsto p_\theta$ is smooth in a neighborhood of θ^* .

(A2) *Local quadratic expansion of \mathcal{L} .* Around θ^* , the cross-entropy admits the second-order expansion

$$\mathcal{L}(\theta^* + \delta) = \mathcal{L}(\theta^*) + \frac{1}{2} \delta^\top F \delta + o(\|\delta\|^2),$$

where F is the Fisher information matrix at θ^* :

$$F := \mathbb{E}_x \text{Cov}_{y \sim p^*(\cdot|x)}[\Phi(x, y)] \in \mathbb{R}^{d \times d},$$

assumed positive definite on the relevant subspace.

(A3) *Local first-order expansion of \mathcal{R} .* For small perturbations δ , the reward admits the first-order expansion

$$\mathcal{R}(\theta^* + \delta) = \mathcal{R}(\theta^*) + g^\top \delta + o(\|\delta\|),$$

for some gradient $g \in \mathbb{R}^d$ characterized in Lemma 2 below under linear softmax setting.

Assumptions (A2)-(A3) are the usual Fisher-geometry expansions of cross entropy and reward around a population optimum in linear soft-max models.

Local dual optimization problem. Based on the assumptions, near θ^* , the MARKTUNE objective can be approximated by

$$J(\theta^* + \delta\theta) \approx \mathcal{R}(\theta^*) + g^\top \delta\theta - \lambda \left(\mathcal{L}(\theta^*) + \frac{1}{2} \delta\theta^\top F \delta\theta \right).$$

The local problem becomes

$$\max_{\delta\theta \in \mathbb{R}^d} g^\top \delta\theta - \frac{\lambda}{2} \delta\theta^\top F \delta\theta := J_{\text{loc}}(\delta\theta). \quad (10)$$

This is a strictly concave quadratic program in parameter space with a unique optimizer.

Lemma 1 (Closed-form optimizer in parameter space). *The unique maximizer of (10) is*

$$\delta\theta^\dagger = \frac{1}{\lambda} F^{-1} g,$$

and the optimal objective value equals $\frac{1}{2\lambda} g^\top F^{-1} g$.

Proof. The objective is $J_{\text{loc}}(\delta\theta) = g^\top \delta\theta - \frac{\lambda}{2} \delta\theta^\top F \delta\theta$. Differentiating and setting the gradient to zero gives the first-order condition

$$g - \lambda F \delta\theta = 0 \quad \Rightarrow \quad \delta\theta^\dagger = \lambda^{-1} F^{-1} g.$$

Positive definiteness of F implies strict concavity and uniqueness. Substituting $\delta\theta^\dagger$ back into J_{loc} yields $J_{\text{loc}}(\delta\theta^\dagger) = \frac{1}{2\lambda} g^\top F^{-1} g$. \square

Lemma 2 (Reward gradient in the linear-softmax model). *Let*

$$\mathcal{R}(\theta) = \mathbb{E}_x \mathbb{E}_{y \sim p_\theta(\cdot|x)}[h(x, y; \xi)],$$

with $h(x, y; \xi)$ as in (8). Then the gradient of \mathcal{R} at θ^* is

$$g := \nabla_\theta \mathcal{R}(\theta)|_{\theta=\theta^*} = \mathbb{E}_x \mathbb{E}_{y \sim p^*(\cdot|x)}[h(x, y; \xi) s(x, y)],$$

where

$$s(x, y) := \nabla_{\theta} \log p_{\theta}(y | x) \big|_{\theta=\theta^*} = \Phi(x, y) - \mu(x), \quad \mu(x) := \mathbb{E}_{y \sim p^*(\cdot|x)}[\Phi(x, y)].$$

Equivalently,

$$g = \mathbb{E}_x \text{Cov}_{y \sim p^*(\cdot|x)}[h(x, y; \xi), \Phi(x, y)],$$

this implies that the reward gradient picks out directions along which the watermark statistic co-varies with the feature representation under the target distribution.

Proof. By definition,

$$\mathcal{R}(\theta) = \mathbb{E}_x \mathbb{E}_{y \sim p_{\theta}(\cdot|x)}[h(x, y; \xi)],$$

and h does not depend on θ . Along a path $\theta(t) = \theta^* + t \delta \theta$ we have

$$\frac{d}{dt} \bigg|_{t=0} \mathbb{E}_{y \sim p_{\theta(t)}(\cdot|x)}[h(x, y; \xi)] = \mathbb{E}_{y \sim p^*(\cdot|x)}[h(x, y; \xi) s(x, y)^{\top} \delta \theta],$$

where $s(x, y) := \nabla_{\theta} \log p_{\theta}(y | x) \big|_{\theta=\theta^*}$. In the linear-softmax model (6),

$$\log p_{\theta}(y | x) = \langle \theta, \Phi(x, y) \rangle - \log \sum_{\tilde{y}} \exp\{\langle \theta, \Phi(x, \tilde{y}) \rangle\},$$

so

$$s(x, y) = \Phi(x, y) - \mathbb{E}_{\tilde{y} \sim p^*(\cdot|x)}[\Phi(x, \tilde{y})] = \Phi(x, y) - \mu(x).$$

Taking expectation over x and reading off the coefficient of $\delta \theta$ gives the claimed gradient expression $g = \mathbb{E}_x \mathbb{E}_{y \sim p^*}[h(x, y; \xi) s(x, y)]$. The covariance form follows by expanding $s(x, y) = \Phi(x, y) - \mu(x)$. \square

Proposition 3 (Second-order CE cost and first-order reward gain). *Let $\delta \theta^{\dagger} = \lambda^{-1} F^{-1} g$ be the optimizer of the local problem (10), with F and g as in (A2) and Lemma 2. Define the MARKTUNE-refined weight $\theta_{\text{MARKTUNE}} = \theta^* + \delta \theta^{\dagger}$ and set $\kappa := \lambda^{-1}$. Then, as $\kappa \rightarrow 0$,*

$$\mathcal{L}(\theta_{\text{MARKTUNE}}) - \mathcal{L}(\theta^*) = \frac{\kappa^2}{2} g^{\top} F^{-1} g + o(\kappa^2),$$

and

$$\mathcal{R}(\theta_{\text{MARKTUNE}}) - \mathcal{R}(\theta^*) = \kappa g^{\top} F^{-1} g + o(\kappa).$$

Consequently, along these directions in the full parameter space the normalized detection statistic experiences a mean shift linear in κ , while the cross entropy deviation from p^* grows only quadratically in κ .

Proof. By the quadratic expansion (A2),

$$\mathcal{L}(\theta^* + \delta) - \mathcal{L}(\theta^*) = \frac{1}{2} \delta^{\top} F \delta + o(\|\delta\|^2).$$

Plugging in $\delta = \delta \theta^{\dagger} = \lambda^{-1} F^{-1} g$ gives

$$\frac{1}{2} (\lambda^{-1} F^{-1} g)^{\top} F (\lambda^{-1} F^{-1} g) = \frac{1}{2 \lambda^2} g^{\top} F^{-1} g = \frac{\kappa^2}{2} g^{\top} F^{-1} g,$$

plus $o(\kappa^2)$.

For the reward, the first-order expansion (A3) with $\delta = \delta \theta^{\dagger}$ gives

$$\mathcal{R}(\theta^* + \delta) - \mathcal{R}(\theta^*) = g^{\top} \delta + o(\|\delta\|) = \lambda^{-1} g^{\top} F^{-1} g + o(\lambda^{-1}) = \kappa g^{\top} F^{-1} g + o(\kappa).$$

This proves the claim. \square

Implications for the improved trade-off. Let $\psi(y; \xi)$ denote the (normalized) GAUSSMARK test statistic computed with the fixed reference model p_θ . Under \mathbf{H}_0 (unwatermarked text), $\mathbb{E}[\psi] = 0$ and the statistic has variance calibrated to yield a level- α test (Proposition 2 in the main text). Under the MARKTUNE-trained weight θ_{MARKTUNE} , the reward increment $\mathcal{R}(\theta_{\text{MARKTUNE}}) - \mathcal{R}(\theta^*)$ corresponds to a mean shift of order κC , where $C = g^\top F^{-1} g > 0$, while the variance of ψ changes only at higher order under standard smoothness assumptions on the statistic, so to first order we may regard it as unchanged. Consequently, for any fixed false positive rate, the true positive rate increases at *first order* in κ , whereas the cross entropy distance to p^* grows only at *second order*.

Soundness of the stylized model and local assumptions. The derivation assumes that the local Fisher geometry at θ^* is well-behaved (so that F is positive definite on the relevant subspace) and that the linear-softmax model (6) adequately captures the first-order behavior of the true language model. In highly over-parameterized language model with wide, flat basins, such local expressivity is often a reasonable approximation [4]. From a geometric viewpoint, $\delta\theta^\dagger$ can be seen as the Riesz representer of the linear functional g under the Fisher metric F ; any parameterization that is locally surjective in the neighborhood of θ^* admits such a direction.

D Implementation Details

In this section, we provide details on the implementation of metrics, baselines, our methods, and the fine-tuning attack. We run the experiments on NVIDIA H200 GPUs.

D.1 Metrics.

For the MAUVE metric, we select samples from the **RealNewsLike** split of **C4** with text longer than 400 tokens, using the first 200 tokens as the model prompt and the next 200 tokens as the human-generated reference. For the **ELI5** dataset, we select samples whose answers exceed 200 tokens and truncate each answer to 200 tokens to serve as the human-generated reference.

In Figures 1 and 5, dashed lines correspond to a bootstrap estimate (500 resamples) of the mean TPR@FPR=1%, and the shaded regions correspond to the 90% confidence interval on the mean estimate.

D.2 Watermarking methods.

Baselines. We use the inference-time KGW watermark [28], which biases the output logits toward a PRF-determined “green list” based on the token prefix. We set the token context length to $k = 4$, the green-list fraction to $\gamma = 0.5$, the bias strength to $\delta = 1$ for KGW-1, and $\delta = 2$ for KGW-2. For Figure 1, we sweep the bias strength δ over the set $\{0.6, 0.7, 0.8, 0.9, 1.0, 1.2, 1.5\}$.

For the non-distortive Gumbel-max watermark [1] and the SynthID watermark [10], we also use a 4-token prefix for fair comparison. For SynthID, we set the number of tournaments to 30, following the recommended default setting.

For KGW-D [18], we distill the logit-based KGW with $\gamma = 0.25$ and $\delta = 1$ to preserve generation quality. Note that we distill the 1-token-prefix KGW variant, since watermarks with longer token prefixes are extremely difficult for the model to learn.

For GAUSSMARK [4], given a vectorized target parameter θ_{wm} with dimension d_r , we first compute its RMS norm $\|\theta_{\text{wm}}\|_{\text{RMS}} = \|\theta_{\text{wm}}\|_{\text{F}} / \sqrt{d_r}$. The watermark key is then sampled as $\xi_\sigma \sim \mathcal{N}(0, \sigma \|\theta_{\text{wm}}\|_{\text{RMS}} \mathbb{I}_{d_r})$. This gives $\mathbb{E} \|\xi_\sigma\|_{\text{F}}^2 \approx \sigma^2 \|\theta_{\text{wm}}\|_{\text{RMS}}^2 d_r$, and thus $\mathbb{E} [\|\xi_\sigma\|_{\text{F}} / \|\theta_{\text{wm}}\|_{\text{F}}] \approx \sigma$. This normalization ensures that the relative perturbation magnitude is directly controlled by σ , making watermark strength easy to tune across different parameter scales and model architectures. We perform a grid search over candidate target parameters and select the up-projection MLP

Table 5: Hyperparameter setting for MARKTUNE on Qwen3-4B.

Model	Qwen3-4B on OpenWebText
Training steps	200
GRPO inner steps	3
Regularization term	Cross-entropy(CE) regularization
Regularization coefficient λ	0.01
Optimizer	AdamW
maximal learning rate	5e-6
Learning rate schedule	Cosine decay with 20 steps linear warmup
Learning rate decay ratio (training steps)	40%
Momentum (β_1, β_2)	(0.9, 0.97)
Group size	8
Prompt batch size	32
Mini batch size	32
Micro batch size	32
Max sampling sequence length	256 tokens
Sampling temperature	0.7
CE batch size	64
CE sequence length	512 tokens
Precision	bfloat16
Data-parallel size	4

Table 6: Hyperparameter setting for MARKTUNE on Llama2-7B.

Model	Llama2-7B on OpenWebText
Training steps	300
GRPO inner steps	3
Regularization term	Cross-entropy(CE) regularization
Regularization coefficient λ	0.005
Optimizer	AdamW
maximal learning rate	4e-6
Learning rate schedule	Cosine decay with 30 steps linear warmup
Learning rate decay ratio (training steps)	40%
Momentum (β_1, β_2)	(0.9, 0.97)
Group size	8
Prompt batch size	32
Mini batch size	32
Micro batch size	32
Max sampling sequence length	256 tokens
Sampling temperature	1.0
CE batch size	64
CE sequence length	512 tokens
Precision	bfloat16
Data-parallel size	4

matrix in layer 28 for Qwen3-4B with $\sigma = 1.0$, and the up-projection MLP matrix in layer 30 for Llama2-7B with $\sigma = 1.2$. For Figure 1, we sweep the perturbation strength σ over the set $\{0.6, 0.8, 1.0, 1.1, 1.2, 1.5, 1.8\}$ for Qwen3-4B and $\{0.8, 1.0, 1.2, 1.3, 1.4, 1.6, 2.0\}$ for Llama2-7B.

Our method. For MARKTUNE, we inherit the target parameter from GAUSSMARK and use $\sigma = 0.6$ for Qwen3-4B and $\sigma = 0.8$ for Llama2-7B to apply a soft activation. For the KL regularization, we use the Qwen3-8B and Llama2-13B as the oracle models, respectively. The GRPO-related hyperparameters are listed in Table 5 and Table 6. For Figure 1, we sweep the number of training steps over the set $\{50, 100, 150, 200, 250, 300, 500\}$ for Qwen3-4B and $\{50, 100, 200, 300, 400, 500, 600\}$ for Llama2-7B.

D.3 Fine-tuning attack.

We fine-tune all models on **OpenWebText** for 1500 steps using the AdamW optimizer with a maximal learning rate of 1×10^{-5} and a cosine decay schedule with 300 warmup steps. We use a sequence length of 512 and a batch size of 64. For LoRA, we set the rank to 8 and the alpha to 16. LoRA is applied to all MLP projection layers as well as to the unembedding layer.

E Supplemental Results on Robustness

In Table 7, we report text perplexity under different attack strategies. The results show that token-deletion and token-substitution attacks substantially degrade generation quality, as indicated by their high perplexity. In contrast, paraphrasing attacks maintain low perplexity and preserve text quality, making them a more realistic and plausible method for watermark removal.

Table 7: Extension of Table 2 with perplexity (PPL) to validate attack plausibility.

Attack	Metric	KGW-1	KGW-2	Gumbel-max	SynthID	KGW-D	GaussMark	MarkTune
Qwen3-4B, T=0.7								
Del-0.2	AUC↑	0.881	0.975	0.993	0.987	0.947	0.908	0.921
	TPR↑	0.330	0.746	0.948	0.890	0.582	0.366	0.484
	PPL↓	20.50	25.19	18.82	19.15	21.23	19.49	19.39
Del-0.5	AUC↑	0.617	0.697	0.778	0.780	0.851	0.622	0.744
	TPR↑	0.040	0.082	0.162	0.094	0.196	0.048	0.068
	PPL↓	98.53	117.25	94.82	94.19	99.95	96.82	94.79
Sub-0.2	AUC↑	0.873	0.986	0.993	0.986	0.939	0.919	0.948
	TPR↑	0.324	0.826	0.922	0.846	0.578	0.384	0.552
	PPL↓	24.71	28.64	21.46	23.06	25.44	23.42	23.17
Sub-0.5	AUC↑	0.638	0.747	0.840	0.834	0.837	0.775	0.783
	TPR↑	0.048	0.106	0.348	0.182	0.190	0.100	0.110
	PPL↓	71.05	80.28	60.34	67.19	72.48	68.96	67.52
Dipper-1	AUC↑	0.771	0.884	0.945	0.941	0.855	0.915	0.977
	TPR↑	0.142	0.372	0.748	0.576	0.274	0.438	0.852
	PPL↓	6.51	7.30	6.07	6.18	6.56	6.24	6.16
Dipper-2	AUC↑	0.573	0.616	0.721	0.700	0.589	0.795	0.851
	TPR↑	0.026	0.038	0.146	0.074	0.030	0.138	0.254
	PPL↓	7.72	8.34	7.81	7.59	7.70	7.80	7.62
Translate	AUC↑	0.831	0.928	0.955	0.968	0.912	0.948	0.973
	TPR↑	0.242	0.552	0.846	0.818	0.404	0.574	0.858
	PPL↓	9.16	11.37	8.33	8.73	9.29	8.95	8.81
Llama2-7B, T=1.0								
Del-0.2	AUC↑	0.853	0.975	0.993	0.979	0.914	0.835	0.928
	TPR↑	0.232	0.712	0.924	0.774	0.410	0.242	0.506
	PPL↓	23.71	27.13	21.66	22.55	23.54	22.86	22.49
Del-0.5	AUC↑	0.581	0.711	0.790	0.777	0.803	0.617	0.783
	TPR↑	0.024	0.060	0.224	0.114	0.148	0.036	0.080
	PPL↓	92.81	105.16	87.05	88.56	95.12	89.98	88.95
Sub-0.2	AUC↑	0.878	0.980	0.993	0.987	0.887	0.853	0.944
	TPR↑	0.300	0.756	0.950	0.862	0.406	0.228	0.578
	PPL↓	22.97	25.89	21.42	22.50	22.84	22.68	22.53
Sub-0.5	AUC↑	0.638	0.772	0.862	0.843	0.759	0.759	0.809
	TPR↑	0.030	0.126	0.296	0.140	0.144	0.098	0.122
	PPL↓	48.50	52.78	44.80	46.69	47.12	46.78	46.51
Dipper-1	AUC↑	0.757	0.862	0.950	0.943	0.814	0.857	0.961
	TPR↑	0.116	0.322	0.700	0.552	0.238	0.240	0.836
	PPL↓	8.33	8.91	7.90	8.11	8.19	8.13	8.09
Dipper-2	AUC↑	0.551	0.614	0.711	0.710	0.590	0.687	0.859
	TPR↑	0.014	0.032	0.148	0.084	0.026	0.060	0.270
	PPL↓	9.34	9.58	8.64	8.97	9.25	9.07	9.02
Translate	AUC↑	0.777	0.922	0.961	0.949	0.889	0.925	0.966
	TPR↑	0.146	0.448	0.796	0.612	0.324	0.436	0.834
	PPL↓	13.27	14.99	11.69	12.68	12.86	12.56	12.47

F Examples of Generated Texts

In this section, we present sample text completions generated by the Qwen3-4B and Llama2-7B models. Prompts are drawn from the **realnewslike** split of the **C4** dataset and truncated to 200 tokens. For Qwen3-4B, we use a sampling temperature of 0.7 to generate 200-token outputs, and for Llama2-7B, we use a temperature of 1.0. Note that the resulting prompts differ slightly between the two models due to differences in their tokenizers. In the examples below, the text under the heading “Base Model” corresponds to a random completion produced by the original, unwatermarked model, while the text under “Watermarked Model” shows a random completion generated by the model trained with MARKTUNE using the hyperparameters detailed in Appendix D.

F.1 Example 1

Input Prompt: Dubai: The Dubai Financial Market (DFM) witnessed another round of selling on Monday as traders remained cautious ahead of a long holidays. The DFM general index closed 0.44 per cent lower at 2,727.41, as it managed to stay above the support level of 2.706 that has proved critical after the gauged bounced back from these levels twice. Emaar Properties closed 1.2 per cent lower at Dh4.74. Emaar shares are struggling to find a bottom as the stock has been trading near to its previous low. A close over Dh4.85 shall be considered bullish, and ignite recovery to Dh4.95/5.20 in the short term, Shiv Prakash, senior analyst with First Abu Dhabi Bank Securities said in a note. Emaar’s movements appear to be concerning at this time of year where investors are expected to be taking positions instead

Qwen3-4B Generations

Base Model: of holding shares ahead of the upcoming holidays, he added. Shares of Emaar had touched Dh4.45 earlier, before recovering to Dh4.50. DFM-listed companies in the real-estate and construction sector declined on the day, with Emaar, Dubai Land Department, Dubai World, Dubai Holding and Dubai Islamic Bank all trading lower. The DFM’s general index has been trading below 2.706 since August 12. The stock index had breached this support level in July, as it rallied from its 13-month low of 2.616, which was recorded on July 12. The index has bounced twice after testing the support level. On the other hand, shares of Al Maktoum International Airport had surged 3.8 per cent to Dh1.084 after the airport operator said on Monday that it has entered into a Memorandum of Understanding (MoU) with the International Air

z-score: -0.6454; p-value: 0.7406; perplexity: 5.0251

Watermarked Model: of selling off. We believe the stock has priced in the worst of the recent troubles and given the firm’s strong fundamentals, we now expect a bounce towards Dh5.20, he said. We continue to expect Emaar’s shares to rally towards Dh5.20 in the next couple of months as the firm has proved resilient in the past. The stock looks cheap given the discount to the firm’s intrinsic value, and we now expect the shares to rally towards Dh5.20 in the next couple of months, he added. The real estate sector was the biggest loser of the day, with the sector index down by 1.2 per cent at 3,124.13. Almarai (ALM) declined 2.2 per cent to Dh5.85, while Alrosa (ARO) shed 1.9 per cent to Dh1.53 and Alshaya (ALY) dropped 1.

z-score: 4.5114; p-value: 3.2187e-06; perplexity: 4.625

Input Prompt: Dubai: The Dubai Financial Market (DFM) witnessed another round of selling on Monday as traders remained cautious ahead of a long holidays. The DFM general index closed 0.44 per cent lower at 2,727.41, as it managed to stay above the support level of 2.706 that has proved critical after the gauged bounced back from these levels twice. Emaar Properties closed 1.2 per cent lower at Dh4.74. Emaar shares are struggling to find a bottom as the stock has been trading near to its previous low. A close over Dh4.85 shall be considered bullish, and ignite recovery to Dh4.95/5.20 in the short term, Shiv Prakash, senior analyst with First Abu Dhabi Bank Securities

Llama2-7B Generations

Base Model: (FASB Securities), said. The stock has traded in a narrow range for almost two years, during which time the stock did gain some momentum but failed to penetrate the key resistance point of Dh4.98/5. Since then, there has been no meaningful progress and the stock price has been in a free fall mode, he said. Emirates Telecommunication Group was the most active stock traded on the index with nearly 9.619 million shares, closely followed by Arabtec with over 8.219 million shares. On value terms, Emaar Properties contributed roughly Dh153.32 million to the market capitalisation, followed by Arabtec with Dh43.25 million and Emirates NBD with Dh20.69 million. In sectoral terms, the real estate sector led the top gainers with a surge

z-score: 0.5016; p-value: 0.3079; perplexity: 5.2253

Watermarked Model: (FASB Securities), told the Gulf News. Dubai Islamic Bank, meanwhile, was another leading index heavyweight to gain ground on Monday. Shares of the bank picked up 0.77 per cent to close at Dh6.42. On the DFM and other markets in the region, we're looking at the 19th [August] as a down day for traders and investors, said Ahmed Saqr, assistant director, financial control department at Abu Dhabi Islamic Bank. After the Eid week, many traders and investors will have just a few days left in August to trade, he added. Investors will take a wait-and-watch approach, he said. Their sentiment towards the markets may turn negative at the beginning of September, because of the US September rates hike talks. This could negatively

z-score: 4.3386; p-value: 7.1526e-06; perplexity: 5.4523

F.2 Example 2

Input Prompt: MADRID: As Cristiano Ronaldo enjoyed his time off at the French Riviera, his Portugal team-mates were busy handing Italy another disappointing result in the UEFA Nations League. Portugal did not need Ronaldo, who skipped international duty to recharge after a busy summer, to beat Italy 1-0 in Europe's newest soccer competition. Elsewhere, Turkey mounted a remarkable comeback from two goals down against Sweden, while Kosovo made history with their first competitive win since being admitted to UEFA in 2016. The European champions easily outplayed Italy, which had opened its Nations League campaign with a disappointing 1-1 home draw against Poland in its first competitive match under coach Roberto Mancini. Andre Silva scored on a counterattack early in the second half to give Portugal the Group 3 win in the top-tier League A. The hosts had several chances to extend their lead at the Stadium of Light in Lisbon, while Italy created little and relied mostly on set pieces. The Nations League gives

Qwen3-4B Generations

Base Model: a fresh impetus to the tournament that replaced the European Championship qualifiers. The top-tier league is divided into four pots, with each group consisting of four teams. The top two teams in each group will qualify for the 2020 European Championship in France. Turkey, which is not currently ranked in the top 20, came back from two goals down to beat Sweden 3-2 at the Group 3 venue in Istanbul. The Swedes took the lead in the 25th minute through a penalty, but the hosts had already equalised a minute later on a goal from a corner. Turkey took the lead through a goal from Ali Kocak, but the Swedes equalised through a Hakan Yakin penalty, before Kocak scored in the 70th minute to make the match up until then a 2-2 stalemate. The hosts took the lead through a goal from Cemre Onay in the 89th minute to win

z-score: 0.9452; p-value: 0.1722; perplexity: 4.9626

Watermarked Model: the teams a chance to warm up for next summer's Euros, where they will face each other. But with Italy's defence vulnerable, the likes of Paulo Dybala and the injured Mario Balotelli were hardly needed. We should have won the game, but we didn't get the best of it, Mancini said after the defeat. This was a good way to start the Nations League, but we now have to find a way to get better because it's not enough to beat Portugal. Italy's next opponents in the group stage are the likes of Poland and Wales, but the 2020 European champions are already planning for the big games after the Nations League ends. We'll start preparing for the next phase of the year, because we know we're going to face some tough opponents in the next few weeks, Mancini said. We'll focus on those games and try to make the most of the opportunities we have. The Italians will also be looking to bounce back

z-score: 4.3033; p-value: 8.4043e-06; perplexity: 5.4245

Input Prompt: MADRID: As Cristiano Ronaldo enjoyed his time off at the French Riviera, his Portugal team-mates were busy handing Italy another disappointing result in the UEFA Nations League. Portugal did not need Ronaldo, who skipped international duty to recharge after a busy summer, to beat Italy 1-0 in Europe's newest soccer competition. Elsewhere, Turkey mounted a remarkable comeback from two goals down against Sweden, while Kosovo made history with their first competitive win since being admitted to UEFA in 2016. The European champions easily outplayed Italy, which had opened its Nations League campaign with a disappointing 1-1 home draw against Poland in its first competitive match under coach Roberto Mancini. Andre Silva scored on a counterattack early in the second half to give Portugal the Group 3 win in the top-tier League A. The hosts

Llama2-7B Generations

Base Model: dominated for most of the game by playing Portugal more openly and allowing more space in midfield, but they struggled to take advantage. Portugal's previous victory over Italy was 1-0 in the Euro 2016 semifinals when it lifted the tournament's trophy. Italy played most of that game with 10 men after defender Giorgio Chiellini received a red card. Portugal was the only one of the 21 European members of the competition which had already played two games in Group 3 prior to the opener against Italy. The host nation, Spain and Poland had one game apiece and will continue the campaign this week. Italy lost its first two fixtures in the Nations League and missed out on qualification for the 2018 World Cup in Russia, while Portugal is one of Europe's major powers. It finished third in

its group at the World Cup, losing

z-score: -1.7278; p-value: 0.9579; perplexity: 5.8205

Watermarked Model: dominated for most of the game by patiently counterattacking when Italy tried to play with the ball. The Portuguese had their most threatening chances when Matteo Politano was sent off after 30 minutes for a rash challenge on Joao Mario outside the penalty area. Ricardo Horta shot wide from a good position. Italy dominated ball play in the midfield and defense after Portugal scored in the 53rd, but lacked the final attacking touch. Portugal, which lost its top spot in the FIFA rankings last week, remained two points above Sweden in Group 2 after both teams began their campaigns. The Portuguese host Sweden in September, while Italy travels to Poland. Sweden opened the match with two goals from former Premier League player Emil Forsberg, who scored in the first and 55th minutes. Sweden looked to have the title in its sights as they pressed for a

z-score: 3.5713; p-value: 0.0002; perplexity: 6.2521

F.3 Example 3

Input Prompt: The New York Times on Thursday printed a special section featuring portraits of nearly every member of the record number of female lawmakers in Congress. A viral Twitter thread from the Times' design editor, Josh Crutchmer, includes a video of the covers the night before publication that has been viewed over 320,000 times as of Thursday morning. The photos, which were taken on Capitol Hill over five days by Times photographers Elizabeth D. Herman and Celeste Sloman, are meant as a testament to what power looks like in 2019, according to the paper. Like the work of Kehinde Wiley, who painted Barack Obama Barack Hussein ObamaChina, Russia, Iran rise in Latin America as US retreats Castro wants to follow Obama's lead on balancing presidency with fatherhood Trump's regulatory rollback boosts odds of a financial crisis MORE's official presidential portrait, these photographs evoke the imagery we are used to seeing in the halls of power, but place people not previously seen

Qwen3-4B Generations

Base Model: occupying them. The photographs are intended to show the power of women in our government, according to a Times source. The Times' print section, which ran the portraits on Thursday, also printed an article titled The 2020 Women's History Month Celebration. The article contains a list of female lawmakers and the causes they represent. The Times also published a companion piece featuring portraits of 12 women in Congress who have taken on more than just their usual roles. The article also included a video of the portraits, which had been viewed over 350,000 times as of Thursday morning, and a list of the women whose portraits appeared in the print section. The women profiled in the article include Rep. Jackie Speier, a California Democrat who has been battling cancer since 2015 and who, as of 2019, is one of only 13 women in Congress who have survived cancer. The article also features Rep. Barbara

z-score: 0.6038; p-value: 0.2729; perplexity: 5.9870

Watermarked Model: in that position. It's the kind of thing the paper has been doing for decades. In 2016, it published a series of its own power portraits featuring the leaders

of every major political party during the presidential primaries. This year, the paper has been highlighting the stories of the women running for president and the women in the other major races. But this year's section is particularly special because it's the first time the paper has managed to get the coverage it deserves for its work. The section is the culmination of a massive effort by the paper's editorial and design teams to make the most of the historic moment. There are so many great stories in this election cycle, but we wanted to make sure we told the ones that matter most, said the paper's executive editor, Dean Baquet. The section is just the beginning of what the paper hopes will be a long-term commitment to telling the stories of women in politics. The paper has already announced plans to launch a new

z-score: 3.5408; p-value: 0.0002; perplexity: 5.0692

Input Prompt: The New York Times on Thursday printed a special section featuring portraits of nearly every member of the record number of female lawmakers in Congress. A viral Twitter thread from the Times' design editor, Josh Crutchmer, includes a video of the covers the night before publication that has been viewed over 320,000 times as of Thursday morning. The photos, which were taken on Capitol Hill over five days by Times photographers Elizabeth D. Herman and Celeste Sloman, are meant as a testament to what power looks like in 2019, according to the paper. Like the work of Kehinde Wiley, who painted Barack Obama Barack Hussein ObamaChina, Russia, Iran rise in Latin America as US retreats Castro wants to follow Obama's lead on balancing presidency with fatherhood Trump's regulatory rollback boosts odds

Llama2-7B Generations

Base Model: of successful Obamacare repeal MORE's official presidential portrait, our intent is to show just how diverse the new Congress is from all perspectives, Crutchmer tweeted. According to The Washington Post, the photos also include Rep. Alexandria Ocasio-Cortez, as well as the first Muslim woman elected to Congress. Rep. Ayanna Pressley, who won her election in Massachusetts and is the seat Ocasio-Cortez will take, is featured as the main photo on the cover, which reads Unity in Action. Rep. Ilhan Omar on Monday became the first Somali-American and one of the first Muslim women to serve in Congress. Lawmakers said upon arriving in Washington that they would be a force multiplier, as Omar said. In a statement to The Hill when photos first came out, Omar said the group is going to be

z-score: 0.3792; p-value: 0.3522; perplexity: 6.2308

Watermarked Model: of nuclear incident MORE for the first time, this project honors women on the national stage, portraying them as they are, Times executive editor Dean Baquet said in a statement. One of the lawmakers, Rep. Deb Haaland Deb HaalandNational Archives to release Trump's passport application, other records on Friday: report Judy Chu is the next chairwoman of the Congressional Asian Pacific American Caucus Nadler's top priority is fighting 'epidemic of corruption in our political system' MORE (D-N.M.) who is the first Native American woman elected to Congress, said the photoshoot reflected the way women have been portrayed for centuries, both in media and in the public realmBaquet was in charge of the paper's decision to use the photo of Rep. Alexandria Ocasio-Cortez (D-N.Y.) in a sk

z-score: 3.6125; p-value: 0.0001; perplexity: 6.2042